Carolina da Silva Carreira

Degree in Cellular and Molecular Biology

Novel fluorescent cell-based sensors for detection of viral pathogens

Dissertation to obtain Master Degree in
Molecular Genetics and Biomedicine

Supervisor: Ana Sofia Coroadinha, PhD, ITQB NOVA/iBET

Juri:

President: Prof. Doutora Maria Alexandra Núncio de Carvalho Ramos Fernandes,
Arguer: Prof. Doutor Pedro Miguel Ribeiro Viana Baptista,
Vogal: Prof. Doutora Ana Sofia de Sousa Valente Coroadinha.

FACULDADE DE CIÊNCIAS E TECNOLOGIA
UNIVERSIDADE NOVA DE LISBOA

November 2018

Carolina da Silva Carreira

Degree in Cellular and Molecular Biology

Novel fluorescent cell-based sensors for detection of viral pathogens

Dissertation to obtain Master Degree in
Molecular Genetics and Biomedicine

Supervisor: Ana Sofia Coroadinha, PhD, ITQB NOVA/iBET

Juri:

President: Prof. Doutora Maria Alexandra Núncio de Carvalho Ramos Fernandes,
Arguer: Prof. Doutor Pedro Miguel Ribeiro Viana Baptista,
Vogal: Prof. Doutora Ana Sofia de Sousa Valente Coroadinha.

November 2018

Novel fluorescent cell-based sensors for detection of viral pathogens

Acknowledgements

The first words of acknowledgement go to my supervisor, Dra. Ana Sofia Coroadinha, for giving me the opportunity to work in the Cell Line Development and Molecular Biotechnology Laboratory, for the supervision and for the availability.

A special acknowledgement to Miguel Guerreiro for the scientific knowledge, constant guidance and valuable help. I learned a lot with you this last year.

To all Animal Cell Technology Unit colleagues, especially those from the CLD&MB for the welcome feeling, knowledge transmitted and help during this last year.

To my master internship colleagues Carolina, João and Julie for all the support, mutual encouragement and moments of joy we shared throughout this year.

Às minhas colegas de Mestrado, Alexandra, Maria e Rita por todo o apoio, união e amizade demonstrados ao longo destes anos que passamos na FCT-UNL. Obrigada meninas.

A toda a minha família, avós, madrinha e tios e um especial agradecimento aos meus pais pelo exemplo, apoio incondicional, incentivo e paciência. Aos meus priminhos cuja chegada veio dar-me esperança e alento nos momentos mais difíceis e àqueles que não sendo família é como se fossem Ana e Pedro obrigada.

À minha grande amiga de sempre Ana Duarte, pelas palavras de apoio e motivação que vieram sempre na hora certa. Obrigada por tudo e que por muitos mais anos estes conselhos me cheguem aos ouvidos e sejam retribuídos.

Resumo

Doenças causadas por vírus são responsáveis por milhões de mortes mundialmente. Contudo, estes são usados no desenvolvimento de biofármacos derivados-virais (BDVs), como vacinas e vetores virais para prevenção/tratamento de doenças. Estas aplicações requerem métodos precisos para quantificação de vírus e vetores-virais. Porém, os métodos atuais não são rápidos, precisos nem demonstram elevado processamento.

Esta tese tem como objetivo desenvolver sensores fluorescentes geneticamente codificados em células para deteção de vírus – VISENSORS. Estes são ativados mediante reconhecimento de sequências de clivagem específicas por proteases virais (PV), permitindo detetar vírus e vetores virais sem gene-repórter. Três estratégias foram desenvolvidas baseadas na fragmentação da proteína verde fluorescente ("split-GFP"), cuja indução de distorção estrutural (DE) inibe a fluorescência: espiral, embutida e circular "split-GFP" VISENSORS. Após proteólise a DE é removida e a fluorescência reposta.

Para cada estratégia, diferentes locais-de-clivagem foram otimizados e seu desempenho avaliado mediante atividade de PV de adenovírus e vírus humano da imunodeficiência tipo 1 (HIV-1) em testes transientes e posteriormente, com VISENSORS expressos estavelmente em células animais, analisando a resposta a infeção viral.

A estratégia espiral de VISENSOR para adenovírus, exibiu desempenho inferior e só foi testada em transiente. As estratégias circular e embutida foram testadas mediante infeção com adenovírus, a primeira exibiu Sinal/Ruído (S/R) baixo (1.6) possivelmente devido a instabilidade do sensor, a última demonstrou desempenho assinalável - S/N de 2.0 - passível de aumento mediante melhoramento da DE.

VISENSORS de HIV-1 foram estabelecidos com sucesso, as estratégias embutida e circular obtiveram semelhantes S/R em transiente.

Este trabalho contribuiu para a otimização de sensores para detetar Adenovírus e HIV-1 sem gene-repórter, pela análise do impacto da DE e sequencias de clivagem, mostrando a relevância destes no desempenho do sensor. A estratégia embutida mostrou potencial, contudo é necessário reduzir o Ruído.

VISENSORS podem ser adaptados a diferentes vírus para sua deteção e quantificação bem como BDVs.

Termos-chave: Biossensores fluorescentes, deteção e quantificação de vírus, sensores baseados em células, adenovírus, vírus humano da imunodeficiência tipo um.

Abstract

Diseases caused by viruses are responsible for millions of deaths worldwide. However, viruses are used for development of virus-based biopharmaceuticals (VBBs), like vaccines and viral vectors to treat/prevent diseases. These applications require reliable methods for virus and viral vectors quantification. Nevertheless, current titration techniques fail to provide fast, reliable methods with high-throughput.

This thesis aimed at developing genetically encoded fluorescent cell-based sensors for virus detection - VISENSORS. These are activated upon recognition by viral proteases (VP) of specific cleavable sequences, allowing detection of label-free virus and viral vectors. Three strategies were developed based on split-Green Fluorescent Protein (GFP) fluorescence inhibition caused by inducing a structural distortion (SD): coiled-coil, embedded and cyclized split-GFP VISENSORS. After VP proteolysis, SD is relieved, and fluorescence is restored.

Different backbones were optimized per strategy, and their performance evaluated under VP activity for detection of Adenovirus and human immunodeficiency virus type one (HIV-1) by transient screenings and latter, stably expressing VISENSORS in mammalian cells and analysing its response to viral infection.

The coiled coil strategy for Adenovirus VISENSOR showed the lowest performance being only tested in transient. The cyclized and embedded strategies were tested upon adenovirus infection, the first exhibited a lower Signal/Noise ratio (S/N) (1.6) possibly caused by sensor instability, the latter showed promising performance - S/N of 2.0 - with room for enhancement through improving SD.

HIV-1 VISENSORS were successfully established, where embedded and cyclized strategies proved similar S/N performances in transient.

This work contributes for the optimization of Adenovirus and HIV-1 label-free sensors, by analysing the impact of SD strategies and VP cleavable sequences, showing these have high impact in sensor performance. Embedded strategy showed potential although further improvements to reduce the Noise are needed

VISENSORS can be adapted to different viruses for detection and quantification of viruses and VBBs.

Keywords: Fluorescent biosensors, virus detection and quantification, cell-based sensors, adenovirus, human immunodeficiency virus type one.

List of Contents

Acknowledgements I

Resumo III

Abstract V

Figures Index IX

Tables Index XI

List of Abbreviations XIII

1. Introduction 1

1.1. An historical perspective of vaccination and gene therapy 1
1.2. Viral titration methods 4
1.2.1. Cell culture base techniques for quantification of infectious virus units 5
1.2.2. Viral nucleic acid detection and quantification methods 5
1.2.3. Flow cytometry 6
1.3. Biosensors 7
1.4. Fluorescent protein biosensors 8
1.5. Green fluorescent protein 8
1.6. Fluorescent cell-based sensors 9
1.7. Biology of adenoviruses 11
1.7.1. Adenovirus protease 12
1.7.2. Adenovirus replication cycle 13
1.8. Biology of lentiviruses 13
1.8.1. HIV-1 protease 14
1.8.2. Lentiviral vectors 15
1.9. Aim and strategy 16

2. Materials and Methods 19

2.1. Plasmids 19
2.2. Coiled coil Split-GFP VISENSORS 19
2.3. Embedded Split-GFP VISENSORS 20
2.4. Cyclized Split-GFP VISENSORS 21
2.5. Proteases 21
2.6. Cloning procedures 22
2.7. Bacterial strains and culture media 22
2.8. Plasmid purification and quality control 23
2.9. Cell lines and culture conditions 23
2.10. Determination of cell concentration and viability 23
2.11. Backbones performance analysis by transient transfection 24
2.12. VISENSORS characterization by Adenovirus infection 25
2.13. Genomic DNA extraction and Real-Time Quantitative PCR 25
2.14. Protein extraction and Western blotting 25
2.15. Flow cytometry data acquisition and analysis 26

3. Results 27

3.1. Backbones performance analysis for Adenoviral VISENSORS in transient screening 27
3.2. eGFP strategy for Adenoviral VISENSORS - eLRGAG backbone characterization by ADV5 infection 29
3.3. cGFP strategy for Adenoviral VISENSORS - cG/LRGAG/G cleavable linker characterization by ADV5 infection 30
3.4. Characterisation of the eGFP and cGFP VISENSORS 31
3.5. HIV-1 protease assessment under transient expression in HEK 293T cells 33
3.6. Backbones performance analysis for HIV-1 VISENSORS in transient screening 35

4. Discussion and conclusions 37

5. References 41

Annexes 49

Figures Index

Figure 1.1 Diseases addressed by gene therapy clinical trials ……2

Figure 1.2 Clinical trials performed using adenoviral or lentiviral vectors ……...…3

Figure 1.3 Vectors used in gene therapy clinical trials …….……3

Figure 1.4 Schematic representation of the ADV replication cycle…….....13

Figure 1.5 Schematic representation of third generation lentiviral vector packaging system …16

Figure 1.6 Schematic representation of the strategies developed for the construction of the VISENSORS…….…17

Figure 2.1 Schematic representation of coiled coil strategy.……..…19

Figure 2.2 Schematic representation of embedded strategy……..……20

Figure 2.3 Schematic representation of the cyclized strategy…… .21

Figure 2.4 Schematic representation of the co-transfection executed to evaluate VISENSORS performance ……..……...24

Figure 3.1 Fluorescence microscopy images of the adenoviral VISENSORS designed with different backbones ……..……..…27

Figure 3.2 Adenoviral VISENSORS Signal/Noise ratios obtained for the different strategies and backbones ……..……28

Figure 3.3 Adenoviral VISENSOR fluorescence microscopy images obtained for the eLRGAG backbone stably expressed in HEK 293 cells ……..……..……...…..29

Figure 3.4 Adenoviral VISENSOR Signal/Noise ratios obtained for the eLRGAG backbone stably expressed in HEK 293 cells ……...……..30

Figure 3.5 Adenoviral VISENSOR fluorescence microscopy images obtained for the cG/LRGAG/G backbone stably expressed in HEK 293 cells …… 30

Figure 3.6 Adenoviral VISENSOR Signal/Noise ratios obtained for the cG/LRGAG/G backbone stably expressed in HEK 293 cells ……..……31

Figure 3.7 HEK 293 cell populations stably expressing the GFPS10, eGFP or cGFP infected with retroviral virus containing the GFPS11 non-distorted……32

Figure 3.8 Values of GFP mean Fluorescence Signal and Noise acquired after HEK 293 cell populations stably expressing the GFPS10, eGFP or cGFP were infected with retroviral virus containing LacZ-GFPS11 non-distorted and respective Signal/Noise ratios …….……...32

Figure 3.9 Relative GFPS11 copy numbers integrated in eGFP and cGFP VISENSOR cell populations……..……33

Figure 3.10 HIV-1 PR activity assessment……..……..……..……34

Figure 3.11 Fluorescence microscopy images of HEK 293T cells transfected with the active or inactive form of HIV-1 Protease 34

Figure 3.12 HIV-1 VISENSORS fluorescence microscopy images obtained for the different backbones and cleavable sequences ……..……...35

Figure 3.13 HIV-1 VISENSORS Signal/Noise ratios obtained for the different backbones tested using the different strategies ……..……..……36

Tables Index

Table 1.1 Duration, costs, human labour, disadvantages and advantages of analysed methods for virus quantification……7

List of Abbreviations

ADA-SCID	Adenosine deaminase deficient-severe combined immunodeficiency
ADV	Adenovirus
ADV5	Adenovirus serotype 5
AIDS	Acquired Immune Deficiency Syndrome
CA	Capsid
CMV	Cytomegalovirus
DMEM	Dulbecco's modified Eagle's Medium
DMSO	Dimetil sulfoxide
DNA	Deoxyribonucleic acid
E. coli	*Escherichia coli*
EMA	European Medicines Agency
EMCV IRES	Encefalomyocaerditis virus internal ribosome entry site
env	Envelope gene
Env	Envelope
FBS	Fetal Bovine Serum
FCM	Flow cytometry
FDA	Food and Drug Administration
gag	Gag polyprotein gene
GFP	Green fluorescent protein
HCV	Human Hepatitis C Virus
HEK	Human embryonic kidney
HIV	Human Immunodeficiency Virus
HPV	Human Papillomavirus
HSV	Herpes Simplex Virus
IF	Immunofluorescence
IN	Integrase
ITR	Inverted terminal repeat
IUPAC	International Union of Pure and Applied Chemistry
LB	Luria Broth media

LTR	Long terminal repeat
MA	Matrix
MOI	Multiplicity of infection
M-PER	Mammalian Protein Extraction Reagent
NC	Nucleocapsid
Npu	*Nostoc punctiforme*
PBS	Phosphate Buffer Saline
PEI	Polyethylenimine
PI	Propidium iodide
pol	Polymerase gene
PR	Protease
pro	Protease gene
PRs	Proteases
PVDF	Polyvinylidene difluoride
pVIc	Cleaved 11 residue peptide from the C-terminus of precursor protein VI
qPCR	Quantitative Polymerase Chain Reaction
Rev	Regulator of expression of viral proteins
RNA	Ribonucleic acid
RPL-22	Ribosomal protein L22
RT-qPCR	Reverse Transcription Quantitative Polymerase Chain Reaction
RV	Reverse transcriptase
SEAP	Secreted alkaline phosphatise
SIN	Self-inactivating
S/N	Signal/Noise
SU	Surface subunit
TAT	Activating regulatory protein
TB	Terrific Broth media
TBS	Tris-Buffered Saline
TCID50	Tissue Culture Infectious Dose 50%
TM	Transmembrane subunit
TP	Terminal protein
VCPE	Viral cytopathic effects

VBBs	Virus-based biopharmaceuticals
VLPs	Virus-like particles
WHO	World Health Organization
WPRE	Woodchuck Hepatitis Virus Post-Transcriptional Regulatory Element

1. Introduction

1.1. An historical perspective of vaccination and gene therapy

Currently we observe a fast spreading of many pathogenic agents worldwide. Diseases are no longer restrained to certain geographic areas. Globalization plays a vital role in the increasing cases of infectious diseases; consequently, prophylactic measures and diagnosis techniques are imperative to control and diminish the spread of infectious agents.

According to the World Health Organization (WHO), in 2015 there were estimated that 2.1 million people became newly infected with human immunodeficiency virus (HIV). Indeed, infectious diseases are one of the leading causes of death worldwide and WHO predicts 13 million deaths attributed to these causes in 2050. Since viruses are the most abundant living entities and can mutate rapidly, evolving with their hosts and sometimes adapting to new host species, infections caused by viruses demand our attention.

Vaccination is one of the most effective public health interventions that allows a reduction in the number of deaths caused by infectious agents. In fact, immunization provided by vaccines has decreased global mortality rates caused by infectious diseases in approximately 3 million people per year (Ehreth, 2003). Therefore, vaccine development is more than ever a field were research and investment needs to be made due to its efficacy.

Traditional vaccines are based on inactivated or attenuated pathogens, but in the present century subunit vaccines, which only contain parts of the pathogen become also available. Due to combined advances in genetic engineering and viral immunology a new type of vaccine that belongs to the subunit vaccines group was developed: the virus-like particles (VLPs) vaccines. These particles are composed by structural viral recombinant proteins that self-assemble, forming a pathogen like structure, which promotes the activation of the host immune system (Rodrigues *et al.*, 2015). There are already several VLP vaccines in the market, such as Gardasil which was approved by the European Medicines Agency (EMA) in 2006. Gardasil is composed by the human papillomavirus (HPV) L1 capsid protein from the HPV types 6,11,16,18,31,33,45,52 and 58; later in 2014 this vaccine was also approved by Food and Drug Administration (FDA).

In the pharma industry, VLPs are part of the field of virus-based biopharmaceuticals (VBBs). This segment includes any virus derived component or virus-based particles, which can be used for therapeutic purposes. Viral vectors used for gene therapy purposes are also VBBs (Rodrigues *et al.*, 2014).

Gene therapy aim is to prevent or treat diseases, by introducing nucleic acids into an individual´s cells or tissues. Such technique can be employed to a wide range of diseases, including cancer, monogenic, infectious and cardiovascular diseases as seen in **Figure 1.1** (Mountain, 2000).

Gene therapy can be performed *in vivo* or *ex vivo*. In the *in vivo* approach the vector is administrated to the patient where it targets the cells and delivers the genetic material while in the *ex vivo* method, patient cells are collected, modified by vector-mediated gene delivery followed by re-insertion of the modified cells into the patient (Wirth, Parker and Ylä-Herttuala, 2013).

To perform the delivery of the therapeutic genes into target cells, different methods can be used: there are the non-viral approaches and the viral vectors (Wirth, Parker and Ylä-Herttuala, 2013). The non-viral approaches can be divided into physical or chemical methods. The first uses physical forces, like electroporation or ultrasounds to temporarily weaken the cell membrane, making it more permeable to the entrance of the genetic material: the latter employs carriers such as nanoparticles or liposomes (Edwards and Baeumner, 2006; Al-Dosari and Gao, 2009). In the earlier days of gene therapy development, non-viral approaches were not as explored as the viral vectors due to their poor gene delivery efficiency when compared to the viral methods (Foldvari *et al.*, 2016).

Viral vectors are non-replicative recombinant viruses, modified to contain a transgene of interest. Their natural ability to infect host cells is what makes them useful to be used as efficient vehicles of genetic material delivery, reason why they sum up to 70% of the vectors used in gene therapy clinical trials (Le Doux *et al.*, 1996; Thomas, Ehrhardt and Kay, 2003; Ginn *et al.*, 2018).

The interest in gene therapy has been unprecedented. Until 2017, nearly 2600 gene therapy clinical trials have been completed, are ongoing or have been approved worldwide. Of those, 65% address cancer, 11.1% focus on inherited monogenic diseases and 7% are about infectious diseases. The distribution of diseases addressed by gene therapy clinical trials is presented in **Figure 1.1**.

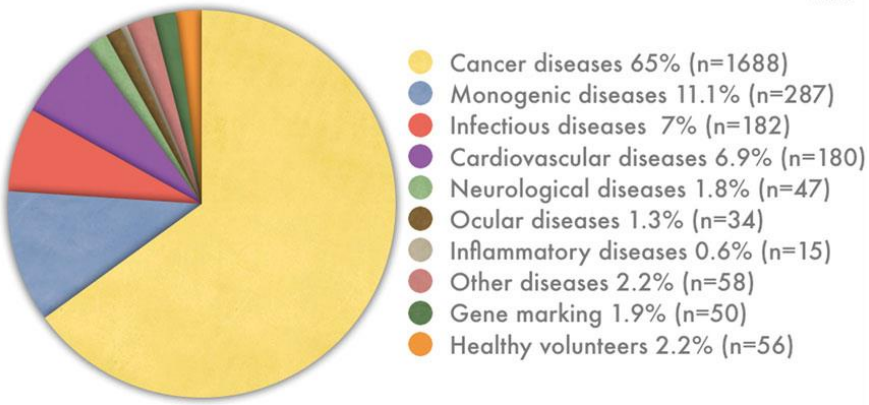

Figure 1.1: Diseases addressed by gene therapy clinical trials. Distribution of diseases targeted by gene therapy clinical trials. Adapted from The Journal of Gene Medicine (Ginn *et al.*, 2018).

Approximately two thirds of the trials performed involve the use of viral vectors and they remain the most used approach for gene therapy.

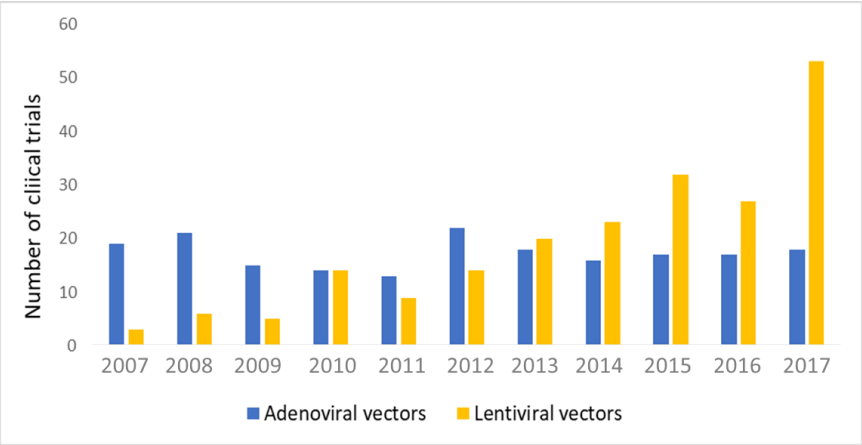

Figure 1.2: Clinical trials performed using adenoviral or lentiviral vectors. Number of gene therapy clinical trials performed from 2007 until 2017. Data collected from: The Journal of Gene Medicine - http://www.wiley.co.uk//genmed/ clinical/ accessed: 2nd November 2018).

The use of lentiviral vectors has seen an increase in the last few years, as seen in **Figure 1.2** and it is expected to keep growing due to their more favourable integration profile, ability to transduce non-dividing cells and because of their lower immunogenicity (Naldini *et al.*, 1996).

The adenoviral vectors historically remain the most used, accomplishing 20.5% of all trials (**Figure 1.3**)**.** They have been tested mainly as cancer therapeutics and, as therapeutic and prophylactic agents against infectious diseases (Ginn *et al.*, 2018).

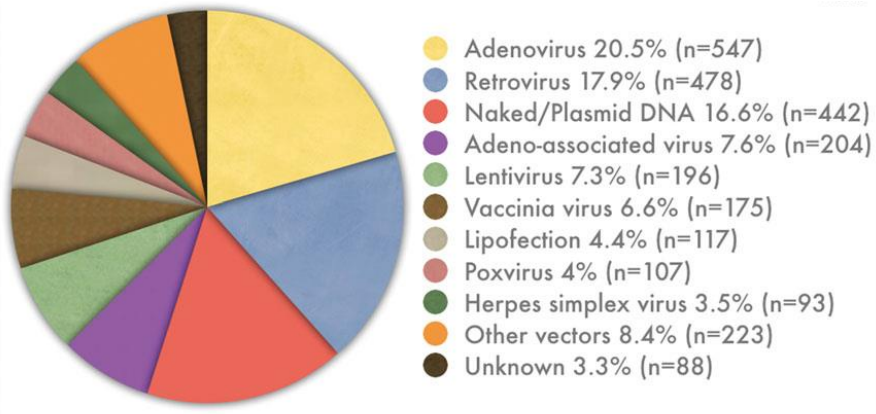

Figure 1.3: Vectors used in gene therapy clinical trials. Distribution of vectors for gene delivery used in gene therapy clinical trials. Adapted from The Journal of Gene Medicine (Ginn *et al.*, 2018).

Adenoviral vectors have the ability to achieve high efficiency of transduction *ex vivo* and *in vivo*, high levels of gene expression even though transient, transduce non-dividing cells and most tissues (Robbins and Ghivizzani, 1998). The drawback associated to these vectors is the insert-size limit of 7.5 kb and the strong immune response induced to the patients.

Due to clinical trials preformed in the last decades, some gene therapy products based on viral vectors have recently reached the market. In 2004 China´s Food and Drug Administration was the first to approve a gene therapy-based product, Gendicine (SiBiono Gene Tech, Shenzhen, China) an adenoviral vector for head and neck cancer. In 2005 it also approved

Oncorine H101 (Sunway Biotech, Shangai, China) an adenoviral vector-based therapy for nasopharyngeal carcinoma (Pearson, Jia and Kandachi, 2004). In 2012, Glybera (uniQure, Amsterdam, Netherlands), an intra-muscular adeno-associated virus vector for the treatment of lipoprotein lipase deficiency was the first human gene therapy product approved by EMA (Watanabe *et al.*, 2015). In 2015 FDA and EMA approved for melanoma immunotherapy, IMLYGIC (Amgen, Thousand Oaks, CA, USA), a live attenuated herpes simplex virus type 1 that expresses an oncolytic granulocyte macrophage colony-stimulating factor (GM-CSF) (Pearson, Jia and Kandachi, 2004). More recently, in 2016 EMA approved Strimvelis (GSK, London, United Kingdom), the first *ex vivo* gene therapy, an hematopoietic stem cell therapy for the treatment of adenosine deaminase (ADA)-deficient severe combined immunodeficiency (SCID) using retroviral vectors encoding adenosine deaminase (Watanabe *et al.*, 2015; Foldvari *et al.*, 2016; Elsanhoury *et al.*, 2017).

Such pharmaceuticals present a need for disease treatment or prevention but are not flawless. In 1999 a patient died because he was incorrectly administrated with a high titer of adenoviral vectors, which led to an immune response culminating in organ failure (Raper *et al.*, 2003; Wirth, Parker and Ylä-Herttuala, 2013). Unfortunate situations like this show the relevance of titration performance for safety improvement in gene therapy protocols.

1.2. Viral titration methods

Research and clinical applications based on viruses and viral vectors require accurate, reliable, and fast methods for viral detection and quantification. For example, gene therapy protocols demand that the number of genome copies administered must be between a defined and reproducible range per target cells and it is crucial to be able to distinguish between infectious and non-infectious particles, since only the ones that possess infectivity are useful for gene therapy purposes. For vaccine development, titration is essential to assess vaccine efficiency (Gates *et al.*, 2009).

The available viral titration methods can be divided into functional and non-functional. The functional methods offer information concerning virus functionality, leading to a direct estimation of the number of infectious viruses, and comprise: the quantification of the viral genome copies in infected cells, that can be measured by Quantitative Polymerase Chain Reaction (qPCR); the assessment of viral cytopathic effects (VCPE) by for example Tissue Culture Infectious Dose 50% (TCID50) and the expression of reporter genes such as fluorescent proteins or beta-galactosidase in infected cells (Gueret *et al.*, 2002).

On the other hand, the non-functional methods provide a quantification of total physical particles in which the non-infective are present. This is not ideal since only the infective particles are useful for gene therapy, often leading to an over-estimation of the virus infectivity because they provide an indirect estimation. These methods include the assessment of the viral transcriptase activity; the determination of the genomic ribonucleic acid (RNA) concentration in

viral preparations by Reverse Transcription Quantitative Polymerase Chain Reaction (RT-qPCR) and the quantification of deoxyribonucleic acid (DNA) in viral preparations by qPCR.

Overall performance, advantages, and disadvantages of these techniques are summarized in **Table 1.1** (Geraerts *et al.*, 2006).

1.2.1. Cell culture base techniques for quantification of infectious virus units

Culture based techniques include the plaque formation assay, which is a classical method used for virus quantification and it has the advantage of not requiring advanced materials nor being expensive. However, this technique can only be used for lytic viruses, is laborious, time consuming since it can take from 5 to 12 days depending on the virus and is operator error-prone. This method of titration is based on the infection of a cell monolayer, with serial viral dilutions. Afterwards cells are fixed and stained so that the plaques formed, corresponding to lysed cells, can be counted and the viral titer determined in plaque forming units per millilitre (PFU/mL) (Fraser and Hink, 1982).

Some viruses can induce morphological changes into the infected cells such as: appearance of inclusion bodies in the nucleus or cytoplasm, establishment of a rounding shape, increase in cell size, or promote the fusion with adjacent cells to form a syncytium. These are examples of VCPE and allows discriminating between infected and non-infected cells.

Since the plaque assay can only be used for virus that produce plaques, alternative procedures were established to determine viral titters based on the VCPE. Among those is the TCID50 that is defined as the dilution of virus required to infect 50% of the cell monolayers. TCID50 is a variation of the previous technique that has the advantage of being performed in 96-well tissue culture plates of permissive cells, thus is more reproducible and has a higher throughput. This assay is based on the observation of VCPE in the infected cells and it consists on the infection of several wells with a different dose of virus in a dilution series. After, the VCPE is accessed, and the dilution of the row were 50% of the wells are considered positive for infection is used for titer calculation. The titer is then reported in infectious units per millilitre (IU/mL). However,TCID50 is still time consuming, laborious, error prone due to operator dependency and it has the drawback of being dependent on the availability of a cell line that responds to infection with a discernible VCPE (Le Doux *et al.*, 1996; LaBarre and Lowy, 2001)

1.2.2. Viral nucleic acid detection and quantification methods

Detection of viruses can be carried out by molecular techniques such as PCR, which can detect and amplify specific viral nucleic acid target sequences. PCR can detect a very low number of viral nucleic acid copies, which make it a very sensitive and sequence specific

method. PCR is performed by the DNA polymerase that exponentially amplifies a DNA target sequence, located between two sequence specific primers in the presence of deoxynucleotide triphosphates for various cycles of temperature variations. PCR is a qualitative method that is combined with an electrophorese in agarose gel to assess the size of the PCR product.

Since PCR is not a quantitative test, other variations of this technique have been developed. An example is the qPCR that uses detection probes to generate a fluorescent signal, which increases proportionally with the increment of the amplification product along each cycle. The concentration of the initial sample is determined by comparison with a calibration curve constructed from a reference gene of known concentration. qPCR is a rapid, sensitive and specific technique, therefore widely used for detection and quantification of viruses, such as HIV, herpes simplex virus (HSV), human hepatitis C virus (HCV), among others (Haramoto *et al.*, 2007; Irshad *et al.*, 2016; Wong *et al.*, 2016). Another variant of the PCR is the RT-qPCR, which might be used for quantification of the viral RNA. This technique comprehends an initial step where the RNA is converted into DNA by a reverse transcriptase. These last two techniques are both rapid, have mid-throughput, are very sensitive and specific, but have the limitation of requiring specific primers for the target sequence and those used cannot form primer dimers.

1.2.3. Flow cytometry

Flow cytometry (FCM) technique is used to analyse physical and chemical characteristics of cells or other particles in suspension as they pass through a measuring apparatus in a single manner. Cell components are fluorescently labelled and then excited by the laser to emit light at varying wavelengths, thus its intensity can be measured by the detector.

For clinical diagnosis purposes, detection and quantification of virus-infected cells can be made by conjugating fluorochrome labelled monoclonal antibodies coupled with FCM. Fluorochrome-labelled monoclonal antibodies to specific HSV antigens and FCM were used to detect and quantify HSV clinical specimens after amplification in tissue culture (McSharry and Costantino, 1990) and cytomegalovirus (CMV) as well as HIV-1 were detected and quantified directly in peripheral blood mononuclear cells of clinical specimens (Mcsharry, 1994; Robillard *et al.*, 1997). However, these methods may depend on tissue culture techniques and on the existence of available fluorochrome-labelled monoclonal antibodies, which are expensive

FCM presents several advantages, such as generating results in rapid fashion with statistical relevance, and even though FCM based assays for viral particle detection does not provide high sensitivity, there are commercial platforms such as the Counter 3100 that allows determining total viral particle concentration with relatively high sensitivities in a few minutes (Yan *et al.*, 2005; Schulze-Horsel, Genzel and Reichl, 2008).

FCM can also be used for the detection and quantification of fluorescent proteins such as Green fluorescent protein (GFP). This is useful when viral vectors have a GFP transgene that

functions as a reporter gene, allowing titration or screening of transduction efficiency (Chou, 1996; Lutz *et al.*, 2005). When using viral vectors that have GFP in their genome it is possible to determine the number of infectious particles, based on the GFP-positive infected cells. However, for clinical purposes viral vectors cannot have reporter genes, such as GFP, due to safety issues (Ansari *et al.*, 2016).

Table 1.1: Duration, costs, human labour, disadvantages and advantages of analysed methods for virus quantification.

	Plaque Assay	TCID50	qRT-PCR	Flow Cytometry
Duration	5-12 days	5-12 days	hours	1 day
Costs	medium	low	high	medium
Human Labour	high	high	medium	low
Disadvantages	Time consuming, Laborious, Subjective counting.	Time consuming, Laborious, VCPE dependent.	Primers availability.	Limited sensitivity.
Advantages	Very high sensitivity	High sensitivity	Fast	Fast

1.3. Biosensors

The International Union of Pure and Applied Chemistry (IUPAC) defines biosensor as “a device that uses specific biochemical reactions mediated by isolated enzymes, immunosystems, tissues, organelles or whole cells to detect chemical compounds usually by electrical, thermal or optical signals”. Biosensors are composed by two basic elements: a bioreceptor, a biological recognition element, that enables specific binding or biochemical reaction with the target analyte; and a transducer, that converts this interaction into a physical measurable phenomenon. The analyte is the substance to be identified and/or quantified. Several types of transducers are used nowadays: electrochemical, thermometric, optical, piezoelectric or magnetic (Damborsky, vitel and Katrlik, 2016).

Biosensors offer some advantages such as producing rapid results or real time analysis, portability, reproducibility and not requiring skilled operators since they provide easy to interpret results. Biosensors can be divided into two groups: direct recognition sensors and indirect detection sensors. The latter are not label free, rely on secondary elements such as enzymes or fluorescent tags for measurements. The direct recognition sensors provide a real-time measurement of the biological interaction, usually using non-catalytic ligands such as cell receptors or antibodies, and do not require additional labelled molecules for detection.

The most common direct detection biosensors are optical biosensors, they generate a signal that is proportional to the concentration of the analyte, usually making use of fluorescent proteins (Damborsky, vitel and Katrlik, 2016).

1.4. Fluorescent protein biosensors

Currently, in the field of optical biosensors it is advantageous to combine the high sensitivity of fluorescence detection with the high specificity provided by ligand-binding proteins. Proteins have evolved to mediate chemical reactions within cells, therefore they can be used as sensors to report the dynamic distribution of specific reactions, monitor reaction kinetics and protein interactions that occur in living cells (Kenneth A. Giuliano, 1998).

Advantages of using proteins as the bioreceptor include the fact that they are easy to manipulate and produce, generally soluble in water and the possibility to improve some of their properties by genetic manipulation. Indeed, different versions of fluorescent proteins were developed with chromophore structure modifications to absorb and emit light at different wavelengths, thus creating new variants of fluorescent protein colours (Heim and Tsien, 1996). Among their numerous applications fluorescent proteins have been used to monitor intracellular dynamics by tagging proteins, evaluate gene expression, used as probes *in vivo* for whole-body imaging for detection of cancer and used in biosensors development (Rizzo, Davidson and Piston, 2009).

Biosensors combined with fluorescent proteins were constructed for example to monitor pH, protein kinase activity and apoptosis (Miyawaki *et al.*, 1997). Fluorescent protein biosensors may exhibit a change in fluorescence excitation or emission wavelengths, fluorescence intensity, fluorescence lifetime of the excited state, or a change from a non-fluorescent to fluorescent state upon activation or vice versa (Seward and Bagshaw, 2009).

Among the different versions of fluorescent proteins, the GFP, which was the first to be discovered by Osamu Shimomura *et al*. is also one of the most used (Shimomura, 1979).

1.5. Green fluorescent protein

The GFP is a soluble monomeric protein that was isolated from the Pacific jellyfish *Aequoria victoria* in the early 1960´s (Seward and Bagshaw, 2009). It is a single chain polypeptide containing 238 amino acid residues, that has 27 kDa and exhibits two peaks of maximum absorption at 395 and 475 nm and excitation at either absorption peak results in emission of green light at 508 nm (Orm *et al.*, 1996).

The protein comprises eleven beta-sheets that are compacted through an antiparallel structure to form a beta-barrel and an alpha-helix that contains the chromophore. Each beta sheet has nine to thirteen residues in length. The first ten beta sheets form the chromophore structure and the eleventh has a conserved Glu 222 that catalysis its maturation (To *et al.*, 2016). Because the chromophore is inside the barrel structure, it is protected from the external environment and this allows GFP to be very stable (Chalfie *et al.*, 1994; Orm *et al.*, 1996).

The GFP protein is widely used as a reporter for gene expression and as a tag for protein localization studies since its fluorescence does not require any substrate or cofactor and because of its stability it can be easily accumulated in cells for detection (Chalfie *et al.*, 1994).

Kamiyama *et al.* (Kamiyama *et al.*, 2016) developed a protein tagging system that is based on the separation of the GFP into two fragments, the GFP S1-10 - from now one referred as GFPS10 - and the GFPS11. The GFPS10 contains the 1-214 amino acids, the GFPS11 is formed by the 215-231 amino acids and it comprises the Glu 222 residue that allows chromophore maturation. These fragments alone do not emit fluorescence; however, they have the natural tendency to suffer transcomplementation, leading to fluorescence emission restoration.

Therefore, the use of a cell-based biosensor that exploits fluorescent proteins, such as GFP are fast non-invasive and easy to perform for virus or viral vectors detection.

1.6. Fluorescent cell-based sensors

Cell based sensors have attracted great attentions because of their high specificity and sensitivity to their targets and optical platforms are fast, sensitive and can be performed without interfering with the normal function of the cells (Fritzsche and Mandenius, 2010). A biosensor that combines the cell-based platform, with the fluorescence provided by a split fluorescent protein and a mechanism for specific viral identification could be used for developing a method for viral titration. The specific mechanism for viral identification could be triggered by the activity of viral proteases (PRs), since they play an important role on viral maturation and infection. Viral PRs have also been scrutinized by pharmaceutical companies, which see them as key targets for antiviral therapies due to their functions on virus life cycle. Therefore, viral PRs are the perfect activating mechanism serving multiple application purposes.

Recently, a few biosensors triggered by PRs activity and aiming to detect viruses or apoptosis (where the cellular protease caspase 3 is a key player) were reported. Iro and co-workers (Iro *et al.*, 2009) developed a cell line for detection of HCV. The fluorescent sensor was based on Lee and co-worker's design (Lee *et al.*, 2003) were an enhanced GFP was fused to the secreted alkaline phosphatise (SEAP) linked by an HCV PR cleavable sequence. Upon HCV infection, its PR recognizes and proteolyzes the cleavage sequence, leading to the release of the SEAP from the fusion protein. The signal peptide present in SEAP N-terminal region can now induce its secretion to the culture medium where it can be detected. Despite being a fast method to detect HCV it cannot be used for determining infectious virus yields.

Also for detection of HCV, Kim and co-workers (Kim *et al.*, 2013) developed a system of detection based on fluorescent reporters' relocalization after infection. The fluorescent reporter contains an HCV PR cleavage sequence and an intracellular translocalization signal sequence. Upon specific cleavage, the peptide signal directs the fluorescent reporter protein from a subcellular organelle to the cytosol or vice versa depending on the translocalization signal. This

system allows the identification of infected cells based on the relocalization of the fluorescent reporter. However, this system cannot be used for virus quantification and it is laborious since it is based on single cell fluorescence microscopy analysis.

Schekhawat and co-workers (Shekhawat *et al.*, 2009) developed a biosensor based on coiled coils for measuring the activity of the tobacco virus PR. The sensor contains a split-firefly luciferase whose half is attached to two coiled coil partners through a cleavable linker, while the other half is connected to another coiled coil identical to one of the pair. The coiled coils are connected to the halves of the reporter through a flexible linker (GGGS). Coiled coils are antiparallel structures made of two to five helices wrapped around each other. Each helix as a periodicity of seven positions labelled from “a” to “g”, the “a” and “d” are hydrophobic and are in the helix interior; “b”, “c”, “e”, “f” and “g” are hydrophilic and constitute the helix exterior. These structures are being explored for their numerous applications for example their value as linker systems, antibody stabilizers and as purification tags (Lupas, 1996; Mason and Arndt, 2004).Transcomplementation is inhibited because the interaction between the two coiled coils connected through the cleavable linker is favoured; however upon PR specific cleavage, the split halves can suffer transcomplementation, restoring the luciferase fluorescence. Nevertheless, this biosensor was only tested for detecting PR activity in complex lysate mixtures and not in living cells.

To and co-workers (To *et al.*, 2016) developed a split-GFP reporter for apoptosis monitoring. Upon caspase cleavage GFP transcomplementation occurs, which increases its fluorescence. The transcomplementation is inhibited because the GFPS11 and the GFPS10 were flanked with E5 and K5 coiled coils and a consensus cleavage sequence (DEVD) for caspase 3 was inserted in split-GFPs. Upon proteolysis, GFPS10 and GFPS11 are unzipped and suffer transcomplementation. This sensor, called ZipGFP, was tested to visualize apoptosis in the living embryos of zebrafish.

Callahan *et al.* developed a biosensor for detection of human immunodeficiency virus type 1 (HIV-1) based on split-GFP transcomplementation after viral PR specific cleavage. A structural distortion was introduced in the GFPS11, which impaired its transcomplementation with the GFPS10. The GFPS11 N- and C-terminal regions were constricted by a stable protein called eglin c connected to a HIV-1 cleavable sequence forcing the GFPS11 to form a loop. Upon HIV-1 PR cleavage the loop like distortion is dissociated and the GFPS10 is available to suffer transcomplementation with the GFPS10 restoring the fluorescence. However, this system was only tested in *E. coli.* (Brian P Callahan, Stanger and Belfort, 2010).

Kanno and co-workers (Kanno *et al.*, 2007) developed a biosensor for detection of caspase 3 activity based on the fluorescence inhibition through a structural distortion caused by the circularization of the firefly luciferase by means of DnaE intein. Inteins are polypeptide sequences that can self-excise during a process called protein splicing, while assuring the re-joining of the two flanking extein sequences by a native peptide bond (Giriat and Muir, 2003; Muralidharan and Muir, 2006). The N- and C-terminal ends of the firefly luciferase were fused with the C- and N-terminal fragments of DnaE intein and a cleavable sequence recognisable by

the caspase 3 was added to the construct. After translation in living cells, the N- and C-terminal ends of the luciferase are ligated and this distortion in the luciferase structure abolishes its bioluminescence activity. After PR cleavage the luciferase changes into an active form and its activity is restored.

Zang and co-workers (Zhang *et al.*, 2013) developed a genetically encoded switch-on fluorescence-based biosensor also for detection of caspase 3 activity. The Venus fluorescent protein was cyclised through the fusion of its N- and C-terminal ends by *Npu* DnaE intein, leading to the inhibition of fluorescence. The cyclised Venus protein contains in its N-terminal end a caspase 3 cleavage site (DEVDG), which upon proteolysis leads to fluorescence emission. This sensor can be applied to detect apoptosis and distinguish it from other types of cell death.

Because many viruses code for a viral PR, necessary to their maturation, these viral proteins can be used to activate a fluorescent sensor genetically encoded in a mammalian cell. These sensors are label-free methods since the virus labelling is not required.

As seen in **Figure 1.3**, adenoviral vectors are the most used in gene therapy clinical trials and lentiviral vectors, whose potential contributed to increase their usage in the last years, would benefit from a fast and label-free method that allow the detection and quantification of their infectious particles.

1.7. Biology of adenovirus

The adenovirus (ADV) were discovered in 1953 by Wallace Rowe and its colleagues, when trying to culture human adenoid tissue *in vitro* (Rowe *et al.*, 1953). ADV belong to de *Adenoviridae* family and they infect a wide range of tissues and species. The human ADV occurs in more than fifty-one serotypes ordered into six species (A – F), according to differences in the guanine-cytosine percentage in their DNA molecule (Waye and Sing, 2010).

ADV infections have worldwide distribution and are responsible for causing gastroenteritis and conjunctivitis, but they are also associated with keratoconjunctivitis, pharyngitis, pharyngoconjunctival fever, and bronchiolitis. Clinical manifestations depend on the serotype and the site of pathology. There are no approved anti-adenoviral therapeutics available even though ADV were recognized to have a significant association with high morbidity and mortality among immunocompromised patients (Lion, 2014).

Adenoviral genome consists in a linear, double-stranded DNA molecule of approximately 35 kb. Each end of the genome has an inverted terminal repeat (ITR), containing a replication origin. A cis-acting packaging sequence required for encapsidation of the DNA molecule is located at one end of the genome.

The genome can be divided into two major transcription regions, the early region, that codes for genes of non-structural proteins and the late region that includes structural protein genes.

E1A, E1B, E2, E3 and *E4* are early region transcript units. The genes here encoded are expressed before DNA replication and regulate the expression of the late region genes. The genes from the late region are generated by alternative splicing of a single transcript and they are expressed from a common major late promotor, shortly after the initiation of DNA replication (Ng and Graham, 2002).

The virion is a nonenveloped particle that encapsidates the DNA molecule. The capsid is composed of three structural proteins: hexon, penton and fiber. The hexon is the major structural component, forming the twenty facets of the icosahedron, also composed by other minor proteins such as IIIa, VI, VIII and IX (Rowe *et al.*, 1953; Reddy and Nemerow, 2014). There are twelve identical fibres each establishing through its N- terminal a non-covalent ligation with the top surface of the penton base (Devaux *et al.*, 1987; Zubieta *et al.*, 2005).

The virus core contains six structural proteins: 23K virion PR, V, VII, Mu, IVa2 and the terminal protein (TP). The latter five are associated with the DNA molecule.

1.7.1. Adenovirus Protease

The PR, more frequently known as Adenain, is a cysteine endopeptidase that is highly conserved amongst the different adenoviruses and synthesised late in viral life cycle.

Adenain structure contains a central mixed five-stranded alpha-sheet surrounded by helices on both sides. Its active site contains a catalytic triplet Cys^{122}-His^{54}-Glu^{71} (Webster, Hay and Kemp, 1993).

The PR is involved in the entry of the virus into the host cell, playing a role in the virus decapsidation and release from the endosome (Greber *et al.*, 1996).

For each adenoviral particle there are between ten to seventy copies of viral PR essential for the assembly of the infective particle, since it is responsible for the cleavage of numerous structural preproteins (IIIa, VI, VIII, VII, Mu and TP) allowing ADV to acquire their mature form in the final phase of viral maturation. The processing of these preproteins is performed in the following consensus cleavage sequences: (M/I/L)XGX↓G and (M/I/L)XGG↓X.

This PR also cleaves in the late phase of the viral infection the cytokeratin 18 and actin leading to cell cytoskeleton dissociation culminating in cell lysis (Chen, Ornelles and Shenk, 1993; Diouri *et al.*, 1996).These events are dependent upon PR activation while in the endosome during uncoating and later by a substrate peptide in the assembled virus (Cotten and Weber, 1995; Greber *et al.*, 1996).

The adenoviral PR is expressed in a nearly inactivated form. The activation reaches its maximum in the presence of two co-factors, an 11-residue fragment called pVIc and the viral DNA (Ding *et al.*, 1996). The pVIc comes from the C-terminus of protein VI – GVQSLKRRRCF - and binds to the PR by hydrogen bonds and a disulphide bond between Cys10 of pVIc and the Cys104 of the PR (Mangel *et al.*, 1993; Webster, Hay and Kemp, 1993).

1.7.2. Adenovirus replication cycle

The ADV replication cycle (**Figure 1.4**) starts upon interaction of the virus fiber protein with the host cell primary receptors, followed by a secondary interaction between the penton base and the cellular integrins (Wickham *et al.*, 1993; Bergelson J. A. Cunningham, G. Droguett, E. A. Kurt-Jones, A. Krithivas, J. S. Hong, M. S. Horwitz, R. L. Crowell and R. W. Finberg., 1997). Afterwards, the virus enters the cell by endocytosis and then escapes across the endosomal membrane, in a pH-dependent step, into the cytoplasm, where its translocated along the microtubule network towards the nucleus, where the transcription of the early genes occurs (Cotten and Weber, 1995). Later, the early proteins are translated in the cytoplasm of the host cell and they re-enter the nucleus where they regulate the transcription of the late viral genes. After the translation of the late genes, its correspondent proteins return to the nucleus where they assemble to form the progeny virions culminating with the virus maturation (Leopold *et al.*, 1998). Approximately 24 hours post-infection, cell lysis is induced, and the virus start being released to infect other cells (Douglas, 2007).

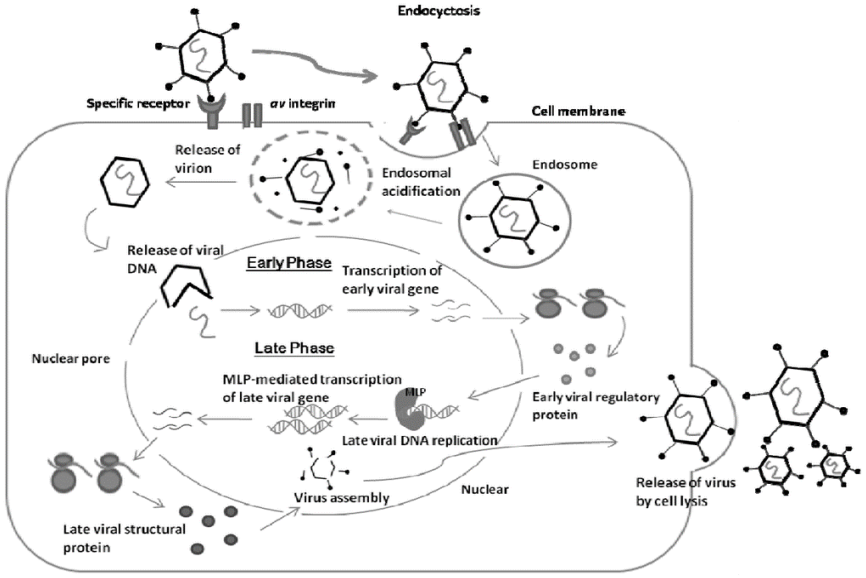

Figure 1.4: Schematic representation of the ADV replication cycle. The virus enters the cell by endocytosis, it promotes endosome acidification which leads to its release. The viral genome enters to the nucleus through a nuclear pore and the transcription of the early genes starts. After translation of the early proteins, they re-enter the nucleus where they regulate the late genes transcription. Late proteins return to the nucleus after translation to assemble, forming the progeny virus, which induce cell lysis to escape the host cell. Adapted from (Waye and Sing, 2010)**.**

1.8. Biology of lentiviruses

The *Retroviridae* family is divided into three subfamilies: *Oncoviridae*, *Spumaviridae* and *Lentiviridae* and the lentiviruses belong to the latter (Matthews, 1979).

Lentiviruses are enveloped virus, whose lipidic bilayer is derived from the infected cell. Their genome is encoded by two copies of linear positive-sense single stranded RNA, which are

reverse transcribed into a double stranded DNA, which is stable integration into the host genome.

The HIV-1 is a lentivirus and the causative agent of acquired immune deficiency syndrome (AIDS). This virus envelope (Env) is composed of two glycoproteins, the surface subunit (SU or gp120) which binds to the cell surface receptors and the transmembrane subunit (TM or gp41), as well as many proteins from the host cell, including major histocompatibility antigens, actin and ubiquitin. Below the envelope there is a protein shell comprising approximately 2000 copies of the matrix (MA) protein (Arthur *et al.*, 1992; Henderson *et al.*, 1992).

The HIV-1 capsid (CA) protein composes the virus capsid and contains two copies of RNA held together as a dimer, stabilized by the nucleocapsid (NC) protein. The capsid also contains the following viral proteins, required for viral infection: protease (PR), reverse transcriptase (RT), integrase (IN) and other accessory proteins (Turner and Summers, 1999).

The HIV-1 genome of about 9-10 kb contains 9 open reading frames that code for structural, enzymatic, regulatory and accessory proteins. One open reading frame encodes the *gag, pol* and *env* genes, that are translated to form large precursor protein that is eventually proteolyzed by the PR into individual proteins. The *gag* gene encodes the Gag polyprotein that is proteolytically processed, during the release of the progeny virions, to generate the MA, CA, NC, and p6 proteins. The *pol* gene comprises the coding regions of the PR, RT, and IN, proteins that are essential for enzymatic functions. Finally, the *env* gene contains an Env precursor (gp160), that is cleaved by PRs into the SU and TM proteins that are structural components of the core and the outer membrane envelope (Frankel and Young, 1998).

Additional sequences encode auxiliary proteins with regulatory functions, such as the trans-activating regulatory protein (Tat) and the regulator of expression of viral proteins (Rev).

The remaining genes code for accessory proteins, like Vif, Nef, Vpr and Vpu, these proteins have functions related with the disease progression or pathogenesis

The long terminal repeat (LTR) is a regulatory sequence of DNA that its present at the 5´and 3´ terminal ends of the provirus. This sequence contains essential elements to drive gene expression, reverse transcription, and integration into the host genome. (Roberts *et al.*, 1990; Watts *et al.*, 2009).

1.8.1. HIV-1 protease

HIV-1 PR was discovered by Gallo and co-workers in 1984. This enzyme is part of the aspartyl PR family and is crucial for the processing of the viral polyproteins and for the maturation of the virus particles. It must therefore cleave the Gag and Gag-Pol polyproteins cleavage sites in the correct order. (Huang, Li and Chen, 2011; Laco, 2015; Tien *et al.*, 2018)

The PR is a homodimer, were each monomer has 99 amino acid residues. A common feature of the aspartic PRs is to possess a conserved Asp-Thr-Gly sequence in each domain contributing to the active site. Each monomer is formed by 9 beta-strands and 1 alpha-helix.

The active site is hydrophobic and shielded from solvent by flexible anti-parallel beta-strands from both monomers that form two flaps to cover the active site (Pearl and Taylor, 1987; Todd, Semo and Freire, 1998; Todd and Freire, 1999; Courtenay *et al.*, 2000).

These flaps assume a semi-open conformation when the enzyme is in a free state and a closed conformation when the ligand is bound to the active site. The substrate is anchored by several hydrogen bonds (Wlodawer *et al.*, 1989; Pearl and Taylor, 1987; Miller *et al.*, 1989; Navia *et al.*, 1989; Coffin, 1995; Todd and Freire, 1999; Tóth and Borics, 2006).

The active site has been mapped and modification of D25 to A, Y, H, or N completely abolishes enzymatic activity (Loeb *et al.*, 1989; Partin *et al.*, 1991; Huang *et al.*, 1995).

The viral PR is synthesized as part of the Gag-Pro-Pol precursor and its autoprocessing happens upon or shortly after virion release. The PR autoprocessing comprises two cleavage reactions that allow the release of the mature PR from the polyprotein.

It has been shown that PR also cleaves host cell cytoskeletal proteins, such as actin, desmin, myosin, tropomyosin, troponin C, vimentin, Alzheimer amyloid precursor protein, and glial fibrillary acidic protein (Shoeman *et al.*, 1990, 1993, 2001; Höner, L Shoeman and Traub, 1992).

The HIV-1 PR is an excellent target for antiviral therapy, since it is crucial to the formation of infectious particles (Karacostas *et al.*, 1993; Wlodawer and Vondrasek, 1998). However, developing efficient inhibitors is difficult because it cleaves different sites that have little or no sequence similarity (Pettit *et al.*, 1991). Therefore, to predict HIV-1 PR cleavage sites, researchers frequently use in-silico approaches (Pettit *et al.*, 1991).

1.8.2. Lentiviral vectors

Lentiviral vectors are based on HIV-1, the best characterized lentivirus. Since the use of a highly pathogenic human virus in gene therapy raises serious biosafety concerns, packaging systems based on these viruses were developed, decreasing the possibility of achieving replication-competent lentiviruses during vector production (Pauwels *et al.*, 2009; Picanco-Castro, Maria de Sousa Russo-Carbolante and Tadeu Covas, 2012).

The third generation (**Figure 1.5**) is the most used, it was developed by Dull and co-workers and it represents the safest packaging system, since it contains only 10% of the viral genome sequence. It is composed of 4 plasmids: a packaging cassette, a rev independent cassette, the envelope cassette and a transfer cassette with the capacity of 8 kb, that will harbour the gene of interest. This split-packaging system increases the number of homologous recombination events necessary to obtain replicative lentiviruses (Dull *et al.*, 1998).

The tat gene from the packaging plasmid was replaced by a chimeric 5'LTR with a heterologous viral promoter, for example from the Cytomegalovirus (CMV), making the lentiviral vector expression independent of Tat. The Rev protein, coded by an independent plasmid, mediates the nuclear export of unspliced mRNA. In addition, a partial deletion of the 3'LTR in

the transgene cassette was performed, leading to transcriptional inactivation of the LTR promoter, after reverse transcription. These vectors are called self-inactivating (SIN) vectors. This inactivation increases safety reducing the possibility of insertional mutagenesis in the adjacent sequences that can lead to transactivation or up-regulation for example of oncogenes (Pauwels *et al.*, 2009).

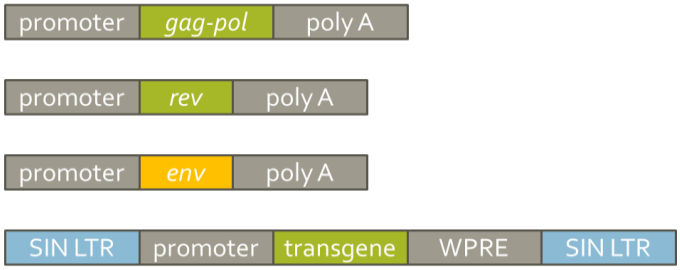

Figure 1.5: Schematic representation of third generation lentiviral vector packaging system. From upper to the lowest: packaging cassette, rev independent cassette, the envelope cassette and the transfer cassette.

1.9. Aim and strategy

The aim of this thesis was to create and characterize a mammalian cell-based fluorescent sensor for detection and quantification of label-free virus. To this end three different strategies, illustrated in **Figure 1.6**, were developed where the GFP was split into two fragments and a structural distortion was induced into one or both fragments aiming to inhibit their transcomplementation and consequently the fluorescence emission.

Many viruses encode viral PRs, needed for their maturation, infectivity and that recognize and proteolyze specific sequences, therefore PR were used as specific agents whose activity is responsible for removing the structural distortions that impairs the transcomplementation of the GFP split fragments, leading to the sensor activation with consequent fluorescence emission.

These sensors were called VISENSORS and in this work two types were developed for detection of different free-label viruses: the adenoviral VISENSORS, constructed for detection of ADV of serotype 5 (ADV5); and HIV-1 VISENSORS developed for HIV-1 detection. ADV5 adenoviral vectors are currently the most used vector in gene therapy clinical trials and HIV-1´s usage is increasing significantly.

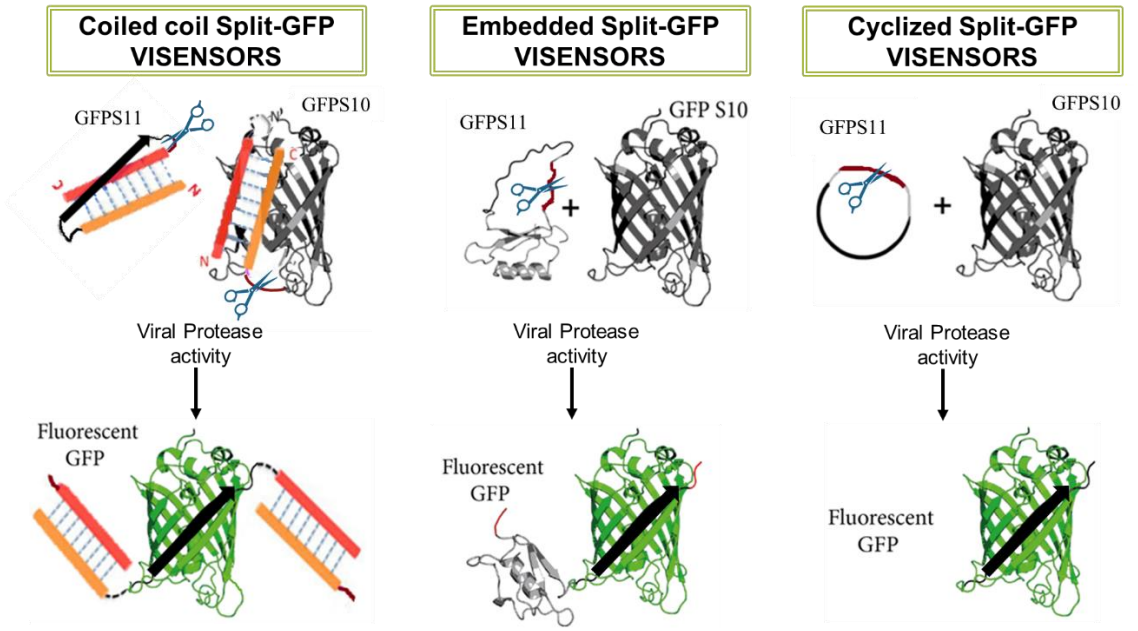

Figure 1.6: Schematic representation of the strategies developed for the construction of the VISENSORS. The **Coiled coil Split-GFP VISENSORS** strategy was based on Shekhawat *et al.*, (2009), where GFPS10 and GFPS11 were flanked by a coiled coil structure. Each constricted GFP split contains a target sequence (red) that upon proteolysis by a viral PR frees each split from the structural distortion resulting in transcomplementation and restored fluorescence. The **Embedded Split-GFP VISENSORS** strategy is a mammalian optimized version of Brian P. Callahan, Stanger and Belfort, (2010) where GFPS11 was embedded as a surface loop into the eglin c protein preventing the transcomplementation of GFP fragments and fluorescence emission. After proteolysis transcomplementation leads to fluorescence emission. The **Cyclized Split-GFP VISENSORS** strategy was based on Zhang *et al.*, (2013) and involves a genetically encoded fluorescent biosensor whose fluorescence is inhibited by circularization of the GFPS11 due to fusion with *Npu* DnaE intein. The fluorescence is reconstituted after viral PR activity proteolyzing a specific cleavage site (represented by the scissors) in the target sequence, removing the circularization and allowing the transcomplementation of the two split-GFP fragments.

Images adapted from To *et al.*, (2016) and Brian P. Callahan, Stanger and Belfort, (2010).

2. Materials and methods

2.1. Plasmids

All plasmids coding for VISENSORS or viral PRs mentioned in this dissertation were constructed using SIN third generation vectors backbones, under the control of a CMV promoter, containing HIV-1 LTR and a Woodchuck Hepatitis Virus Post-Transcriptional Regulatory Element (WPRE) to stabilize the viral RNA and to increase transgene expression in mammalian cells. These plasmids were kindly provided by Miguel Guerreiro (ACT Unit iBET/ITQB NOVA, Oeiras, Portugal). *pRRLSIN.hPGK.eGFP.WPRE* is the original plasmid from which they were derived and it was kindly provided by Dr. Didier Trono through Addgene plasmid repository (plasmid #12252) (Addgene, Cambridge, Massachusetts, U.S.A.).

The parental plasmids *pRRLSIN.CMV.GFPS10.IRES.Zeo.WPRE.v2* and *pRRLSIN.CMV.GFPS10.IRES.Puro.WPRE.v2* used for the development of the VISENSORS strategies are under the control of a CMV promoter and an encefalomyocaerditis virus internal ribosome entry site (EMCV IRES) to drive the expression of the resistance genes: zeocin or puromycin.

Primers and templates for all the plasmids constructed in this work are listed in **Table A.1** in Annexes.

2.2. Coiled coil Split-GFP VISENSORS

This strategy utilizes two plasmids one encoding the GFPS10 fragment that was flanked with a coiled coil E5-K5 sequence (Shekhawat *et al.*, 2009): *pRRLSIN.CMV.ccGLRGAG-GFPS10* and another plasmid: *pRRLSIN.CMV.ccGLRGAG-GFPS11* encoding the GFPS11 fragment also flanked with a coiled coil E5-K5 sequence. Between each coiled coil sequence, a backbone was inserted - LRGA↓G, arrow denoting scissile bond - able to be recognized and proteolyzed by the adenoviral PR.

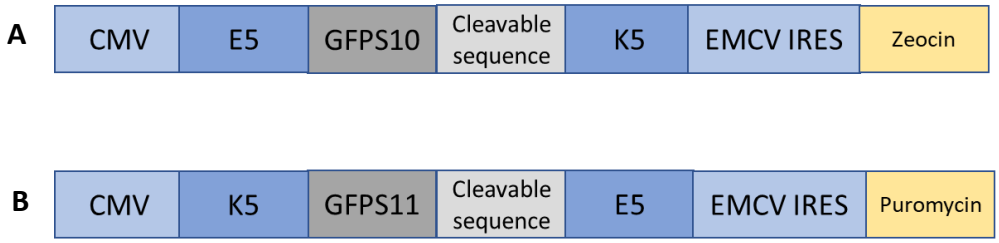

Figure 2.1 Schematic representation of coiled coil strategy. The E5-K5 coiled coils flank each split-GFP and a cleavable sequence under the control of the CMV promoter. The EMCV IRES is promoting the expression of the antibiotic resistance genes: zeocin and puromycin. **A** illustrates the plasmid construction containing the GFPS10 split-GFP and **B** represents the plasmid construction containing the GFPS11 split-GFP.

2.3. Embedded Split-GFP VISENSORS

For this strategy two plasmids are required, one coding for the GFPS10 fragment *pRRLSIN.CMV.GFPS10.IRES.Zeo.WPRE.v2* plasmid and another plasmid coding for the GFPS11 fragment containing a specific backbone recognized by the viral PR.

The GFPS11 fragment was embedded into an Eglin c protein and is encoded into a plasmid derived from the *pRRLSIN.CMV.GFPS10.IRES.Puro.WPRE.v2* where the GFPS10 was replaced by the GFPS11 plus the respective backbone.

For the adenoviral VISENSORS, the GFPS11 fragment were constructed with two different backbones: plasmids *pRRLSIN.CMV.eLRGAG.IRES.Puro.WPRE* and *pRRLSIN.CMV.eGLRGAGG.IRES.PURO.WPRE* comprising the backbones LRGA↓G and G/LRGA↓G/G, respectively.

For the HIV-1 VISENSORS were developed three different GFPS11 comprising the backbones: GIF↓LET, GSGIF↓LETSL reported as the synthetic most efficiently cleaved peptide site (Beck *et al.*, 2000) and the natural cleavage sequence IRKIL↓FLDG,(Miklo *et al.*, 2006) respectively: pRRLSIN.CMV.eGIFLET.IRES.PURO.WPRE , pRRLSIN.CMV.eGSGIFLETSL.IRES.PURO.WPRE and pRRLSIN.CMV.eIRKILFLDG.IRES.PURO.WPRE.

During this thesis, plasmid *pRRLSIN.CMV.eGSGIFLETSL.IRES.PURO.WPRE* was constructed. The N- and C-terminal fragments of eglin c as well as the GFPS11 sequence were amplified through PCR from the pUC57.eLRGAG-GFPS11 plasmid, with primers mutating LRGAG cleavage sequence to GSGIFLETSL. This insert was cloned into the *pRRLSIN.CMV.GFPS10.IRES.Puro.WPRE.v2* plasmid (previously constructed by Miguel Guerreiro (ACT Unit iBET/ITQB NOVA)) opened with NheI and BamHI.

For pRRLSIN.CMV.eIRKILFLDG.IRES.PURO.WPRE construction a synthetic construct insert (Integrated DNA Technologies,Ink, Skokie, Illinois, USA) containing the eIRKILFLDG-GFPS11 was cloned into the pRRLSIN.CMV.GFPS10.IRES.Puro.WPRE.v2 plasmid opened with NheI and BamHI.

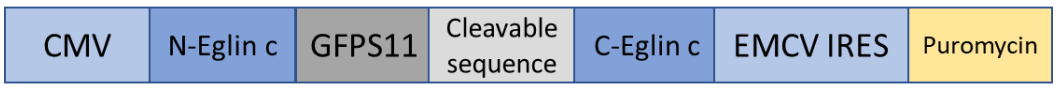

Figure 2.2: Schematic representation of embedded strategy. Under the control of the CMV promoter the N- and C-terminal ends of the Eglin c protein are flanking the GFPS11 and the cleavable sequence. The EMCV IRES is promoting the expression of the puromycin resistance gene.

2.4. Cyclized Split-GFP VISENSORS

The GFPS10 fragment for this strategy is encoded by the plasmid *pRRLSIN.CMV.GFPS10.IRES.Zeo.WPRE*.v2. The GFPS11 fragment was cyclized and the backbone sequence was added.

For the adenoviral VISENSORS three GFPS11 were created containing three different backbones, resulting in the following plasmids: *pRRLSIN.CMV.cLRGAG.IRES.PURO.WPRE, pRRLSIN.CMV.cGLRGAGG.IRES.PURO.WPRE, pRRLSIN.CMV.cGGLRGAGGG.IRES.PURO.WPRE* comprising the following backbones: LRGA↓G, G/LRGA↓G/G and GG/LRGA↓G/GG respectively.

For the HIV-1 VISENSORS three GFPS11 were developed with three different backbones GIF↓LET, GSGIF↓LETSL and *IRKIL↓FLDG* respectively: *pRRLSIN.CMV.cGIFLET.IRES.PURO.WPRE*, *pRRLSIN.CMV.cGSGIFLETSL.IRES.PURO.WPRE* and *pRRLSIN.CMV.cIRKILFLDG.IRES.PURO.WPRE* plasmids.

During this thesis, plasmid *pRRLSIN.CMV.cIRKILFLDG.IRES.PURO.WPRE* was constructed: the synthetic construct insert (Integrated DNA Technologies,Ink) containing the cIRKILFLDG-GFPS11 was cloned into the *pRRLSIN.CMV.GFPS10.IRES.Puro.WPRE.v2* plasmid opened with NheI and BamHI.

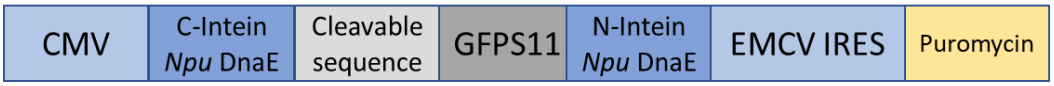

Figure 2.3: Schematic representation of the cyclized strategy. Under the control of the CMV promoter, the C- and N-terminal ends of the *Npu* DnaE intein are flanking the GFPS11 and the cleavable sequence. The EMCV IRES is promoting the expression of the puromycin resistance gene.

2.5. Proteases

The PR used for assessing the adenoviral VISENSORS performance was encoded in the *pRRLSIN.CMV.Adenain-MVGLG-VIc.IRES.ZEO.WPRE* plasmid.

pMDLg/pRRE is a third-generation lentiviral packaging plasmid used to produce lentiviral vectors. Since it encodes the HIV-1 PR, it was used for the transient screening of the HIV-1 VISENSORS. This plasmid was kindly provided by Dr. Didier Trono through Addgene plasmid repository (plasmid #12251).

In this thesis work, the plasmid containing the HIV-1 PR fused to an mCherry was constructed following Konvalinka *et al.*, (2001). For its construction (*pRRLSIN.CMV.mCherry.HIV1Pr.WPRE*) the mCherry and the HIV-1 PR were amplified by PCR from the *pPuro*.m*Cherry* and *pMDLg/RRE* plasmids respectively and both inserts were cloned into the *pRRLSIN.CMV.GFPS10.IRES.Zeo.WPRE* plasmid opened with NheI and SalI.

As control, an inactive PR was constructed, containing the D25N mutation that consists in the replacement of the 25th amino acid from an aspartic acid to an asparagine, since this position is a key point in the active site of the enzyme. The *pRRLSIN.CMV.mCherry.HIV1PrD25N.WPRE* plasmid contains the inactive HIV-1 PR and for its construction the mCherry and the HIV-1 PR with the D25N mutation were amplified by PCR from the *pPuro.mCherry* and *pMDLg/RRED25N* plasmids respectively and cloned in the *pRRLSIN.CMV.GFPS10.IRES.Zeo.WPRE.v2* plasmid opened with NheI and SalI. p*MDLg/RRED25N* plasmid was obtained through point mutation of the *pMDLg/pRRE* plasmid as described in Tomás *et al.*, (2018)

2.6. Cloning procedures

All PCR reactions were performed in Biometria T3 Personal Thermocycler (Biometria, Göttingen, Germany) using Phusion High-Fidelity DNA Polymerase (Clontech Laboratories, Inc., Mountain View, CA, U.S.A.) and appropriate PCR conditions for each fragment as suggested by the manufacturer.

The restriction reactions were performed using enzymes (New England Biolabs, Ipswich, MA, U.S.A.) with the proper buffer according to the manufacturer's instructions.

The restriction fragments were isolated on agarose gels (NZYTech, Lisbon, Portugal) and visualized using GelDoc XR+ system (Bio-Rad, Hercules, CA, U.S.A.) by adding 0.05 µL/mL RedSafe Nucleic Acid Staining Solution (INtRON Biotechnology, South Korea) to the gel.

Generated fragments by PCR reactions were isolated in 0.7% or 2% (w/v) agarose gels (NZYTech) and purified with illustra GFX PCR DNA and Gel Band Purification Kit (GE Healthcare, Little Chalfont, U.K.).

Cloning reactions were performed using In-Fusion HD Cloning Kit (Clonetech, Laboratories, Inc.) following manufacturer's instructions. Primers and templates for all the plasmids constructed in this work are listed in Table A.1 in Annexes.

2.7. Bacterial strains and culture media

Constructed plasmids were produced using *Escherichia coli* (*E. coli*) Stellar (Clontech Laboratories, Inc.) and One Shot Stbl3 (Invitrogen, Carlsbad, CA, U.S.A.) competent cells. Transformation procedures were performed under the manufacturer's instructions. The liquid and agar cultures were performed with Terrific Broth media (TB) and Luria Broth media (LB) (InvivoGen, San Diego, CA, U.S.A.), respectively, supplemented with the appropriate antibiotic for bacteria selection (Ampicillin).

2.8. Plasmid purification and quality control

Plasmid purification was performed at small-scale (yields up to 20 µg of DNA) using GeneJET Plasmid Miniprep Kit (Thermo Scientific, Waltham, MA, U.S.A.) and at large-scale (yields up to 500 µg of DNA) using Genopure Plasmid maxi Kit (Roche Applied Science, Penzberg, Germany), following the manufacturer's instructions.

Working bacteria banks for each plasmid were generated and stored at -20 ºC in 20% (v/v) glycerol (Sigma-Aldrich, St. Louis, MO, U.S.A.).

DNA concentration was determined using Nanodrop 2000C Spectrophotometer (Thermo Scientific). Plasmid purity was assessed by measuring the absorbance ratios at 260nm/280nm and 260nm/230nm.

All plasmids constructed in this work were sequenced by Sanger sequencing using GATC Biotech services (Constance, Germany).

2.9. Cell lines and culture conditions

Human embryonic kidney 293 cells (HEK 293) (ATCC CRL-1573) is a cell line that continuously expresses of the *E1* ADV5 gene since it was derived from human embryonic kidney cells transfected with fragments of mechanically sheared ADV5 DNA (Louis, Evelegh and Graham, 1997).

This cell line was used to establish a cell population stably expressing GFPS10 and GFPS11 VISENSOR's, either cGFP or eGFP strategies.

HEK 293T (ATCC, American Type Culture Collection, CRL-11268) is a cell line derived from HEK 293 cells, expressing the large T antigen of SV40 and was used for the transient protocols.

Cells were cultured in Dulbecco's modified Eagle's Medium (DMEM) (Gibco, Carlsbad, CA, U.S.A.), supplemented with 10% (v/v) Fetal Bovine Serum (FBS) (Gibco) and maintained at 37 °C in a humidified atmosphere with 8% CO_2. All cells were cultured under adherent conditions.

For establishing working cell banks, cells lines were frozen in a cryopreservation solution of FBS containing 5% (v/v) of Dimethyl Sulfoxide (DMSO) (Sigma-Aldrich) and stored at -80 °C.

2.10. Determination of cell concentration and viability

Cell concentration and viability were assessed by the trypan blue exclusion assay, using a 0.1% (v/v) Trypan Blue (Sigma-Aldrich) solution in Phosphate Buffer Saline (PBS) (Gibco). Cell counting was performed in a Fuchs-Rosenthal hemocytometer (Marienfeld-Superior, Lauda-Königshofen, Germany) using an inverted microscope (Olympus).

2.11. Backbones performance analysis by transient transfection

Initial characterization of the VISENSORS' performance was evaluated through transient co-transfection (**Figure 2.4**). For that, HEK 293T cells were seeded at 8×10^4 cells/cm^2 in 24 well plates.

Twenty-four hours after the seeding, transfection was performed using polyethylenimine (PEI) (Polysciences, Inc., Warrington, PA, U.S.A.) at 1:1.5 (w/w) ratio of DNA:PEI. A total of 5 µg of total DNA per million of cells was used. For the screening of adenoviral VISENSOR´s backbones, cells were transfected with three plasmids per condition: GFPS10, GFPS11 (cGFP, eGFP and ccGFP strategies) and either with the adenoviral PR (Signal) or mCherry (Noise). Similarly, for the screening of the HIV-1 VISENSOR´s backbones, cells were transfected with three plasmids per condition: GFPS10, GFPS11 (cGFP and eGFP strategies) and either the HIV-1 PR (Signal), or with mCherry (Noise). The PEI transfection solution was added to the plasmid mix solution, with both solutions prepared in serum-free DMEM. After 13 minutes of incubation at room temperature, the transfection solution composed by the mixture mentioned above was added to the cells.

Forty-eight hours after transfection cells were analysed by fluorescence microscopy using a Leica DMI6000 inverted microscope (Leica, Wetzlar, Germany). Cells were then harvested and GFP fluorescence intensity was analysed by FCM (CyFlow Space, Sysmex Corporation, Norderstedt, Germany).

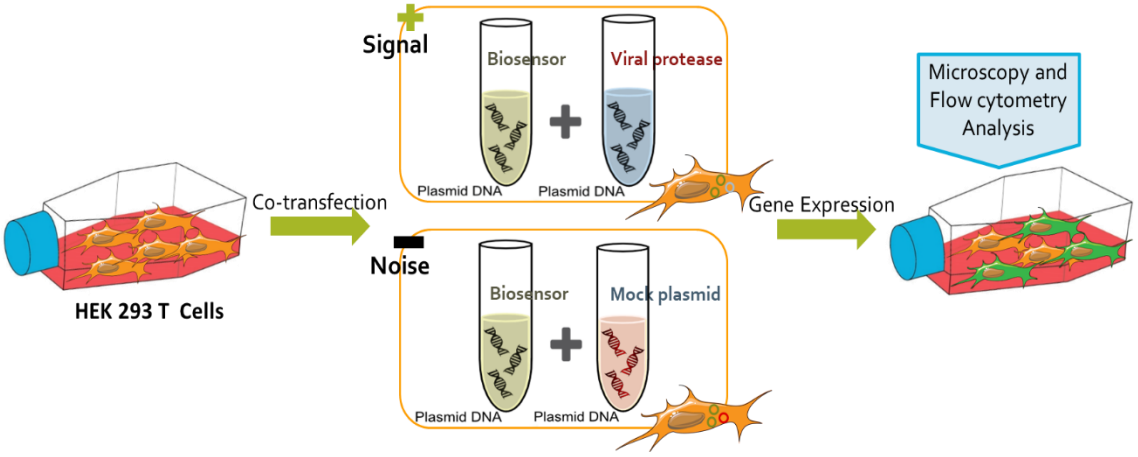

Figure 2.4: Schematic representation of the co-transfection executed to evaluate VISENSORS performance. HEK 293T cells were co-transfected either with plasmids encoding the GFPS10, GFPS11 and the viral PR or with 3 plasmids containing the GFPS10, GFPS11 and a mock plasmid (mCherry). After 48 hours, cells' fluorescent emission was analysed through fluorescent microscopy and flow cytometry.

2.12. VISENSORS characterization by Adenovirus infection

HEK 293 cells stably expressing the VISENSORS (backbones cG/LRGAG/G or eLRGAG) were seeded at $1x10^5$ cells/cm^2 in 24 well plates. Twenty-four hours after, culture media was removed, and cells were infected with a recombinant *E1* deleted strain of ADV serotype 5 expressing a gene of interest for vaccination purposes (provided by Dr. Geneviève Libeau, CIRAD-UMR Contrôle des Maladies, Montpellier, France) at a multiplicity of infection (MOI) of 5 in 0.2 mL of fresh non-supplemented DMEM. After 1 hour of incubation with mild agitation at 37 ºC in a humidified atmosphere with 5% CO_2, 0.3 mL of supplemented DMEM were added.

At the given time points (0, 24, 48 and 72 hours after infection) cells were analysed by fluorescence microscopy using a Leica DMI6000 inverted microscope (Leica). Cells were then harvested and its GFP fluorescence intensity was analysed by a flow cytometer (CyFlow Space).

2.13. Genomic DNA extraction and Real-Time Quantitative PCR

Genomic DNA was extracted using DNeasy Blood & Tissue Kit (Qiagen, Hilden, U.S.A.) according to the manufacturer's instruction and stored at -20 °C.

Real-Time qPCR was performed using LightCycler 480 SYBR Green I Master (Roche Applied Science) according to the manufacturer's instructions on a LightCycler 480 Real Time PCR System (Roche Applied Science). Relative copy numbers for the LTR and posttranscriptional regulatory element of WPRE sequences were calculated using the $2^{-\Delta\Delta CT}$ method and ribosomal protein L22 (RPL-22) was used as reference gene. Primers used for RT-qPCR are listed in **Table A.2** in Annexes.

2.14. Protein extraction and Western blotting

To confirm HIV-1 PR activity, HEK 293T cells were seeded at a 7×10^4 cells/cm^2 in 75 cm^2 tissue culture flasks. After 24 hours, cells were transfected with plasmids containing the active form of the HIV-1 PR fused with the mCherry *(pRRLSIN.CMV.mCherry.HIV1Pr.WPRE*) or with the inactive form that has the D25N mutation also fused with mCherry: (*pRRLSIN.CMV.mCherry.HIV1PrD25N.WPRE*). Cells were harvested 24 and 48 hours post transfection, pelleted at 300 × g for 10 minutes at 4 ºC, and then washed with PBS. Cells were lysed in 100 µL Mammalian Protein Extraction Reagent (M-PER) (Thermo Scientific) per $3x10^6$ cells. cOmplete™ EDTA-free Protease Inhibitor Cocktail (Roche Applied Science) was added to the M-PER. The mixture was vortexed, placed at 4 ºC for 10 minutes and vortexed again. Extracts were clarified by centrifugation at >14000 × g for 10 minutes and finally, samples were

frozen at -20 ºC. Total protein quantification was performed with Pierce™ BCA Protein Assay Kit (Thermo Scientific), according to manufacturer's instructions.

NuPAGE® electrophoresis system (Invitrogen) was used for protein electrophoresis separation, performed under denaturing conditions. Ten µg of total protein were loaded into each well. Samples were resolved on a 4%-12% (w/v) Bis-Tris gel with MOPS SDS Running Buffer, at 180 V for 40 minutes. Protein transfer into polyvinylidene difluoride (PVDF) membrane was performed in Trans-Blot Turbo Transfer System (Bio-Rad) according to manufacturer's instructions. Membranes were blocked with blocking solution 0.1% (w/v) Tween 20 (Sigma-Aldrich) and 5% (w/v) skim milk powder (Sigma-Aldrich) in Tris-Buffered Saline (TBS) (Sigma-Aldrich), for 1 hour at room temperature. Rabbit polyclonal anti-mCherry (AB356482) (Millipore Corporation, Temecula, CA, U.S.A.) and mouse monoclonal anti-α-tubulin (T6199) (Sigma-Aldrich) primary antibodies were diluted 1:2000 and 1:5000, respectively, in blocking solution and incubated with membranes overnight. After washing with 0.1% (w/v) Tween 20 in TBS, membranes were incubated with secondary antibodies: Amersham ECL Anti-Mouse IgG, Horseradish Peroxidase-Linked Species-Specific Whole Antibody (NA931) and Amersham ECL Anti-Rabbit IgG, Horseradish Peroxidase-Linked Species-Specific Whole Antibody (NA934), (GE Healthcare) diluted 1:5000 in blocking solution for 2 hours at room temperature.

Chemiluminescence detection was performed by incubating the membranes with Amersham ECL Prime Western Blotting Detection Reagent (GE Healthcare), according to manufacturer's instructions, and analysed with ChemiDoc XRS System (Bio-Rad).

2.15. Flow cytometry data acquisition and analysis

Signal refers to the GFP geometric mean fluorescence intensity measured when the sensor is activated by a viral PR, either upon transient transfection of the PR or upon viral infection. Noise refers to the GFP geometric mean fluorescence intensity measured when the sensor is not active, upon transient transfection with a mock plasmid, that contains the mCherry reporter, or in non-infected cells stably expressing the sensor.

For the Signal/Noise (S/N) ratio calculations, total fluorescence (TF) was considered by having into account the number of fluorescent cells: (Signal x Number of fluorescent cells)/ (Noise x Number of fluorescent cells).

3. Results

3.1 Backbones performance analysis for Adenoviral VISENSORS in transient screening

To obtain a fluorescent cell-based biosensor for detection of label-free adenoviruses, three different strategies were developed - ccGFP, eGFP and cGFP - with several backbones for the GFPS11 being tested, using the LRGA↓G cleavable sequence as starting point.

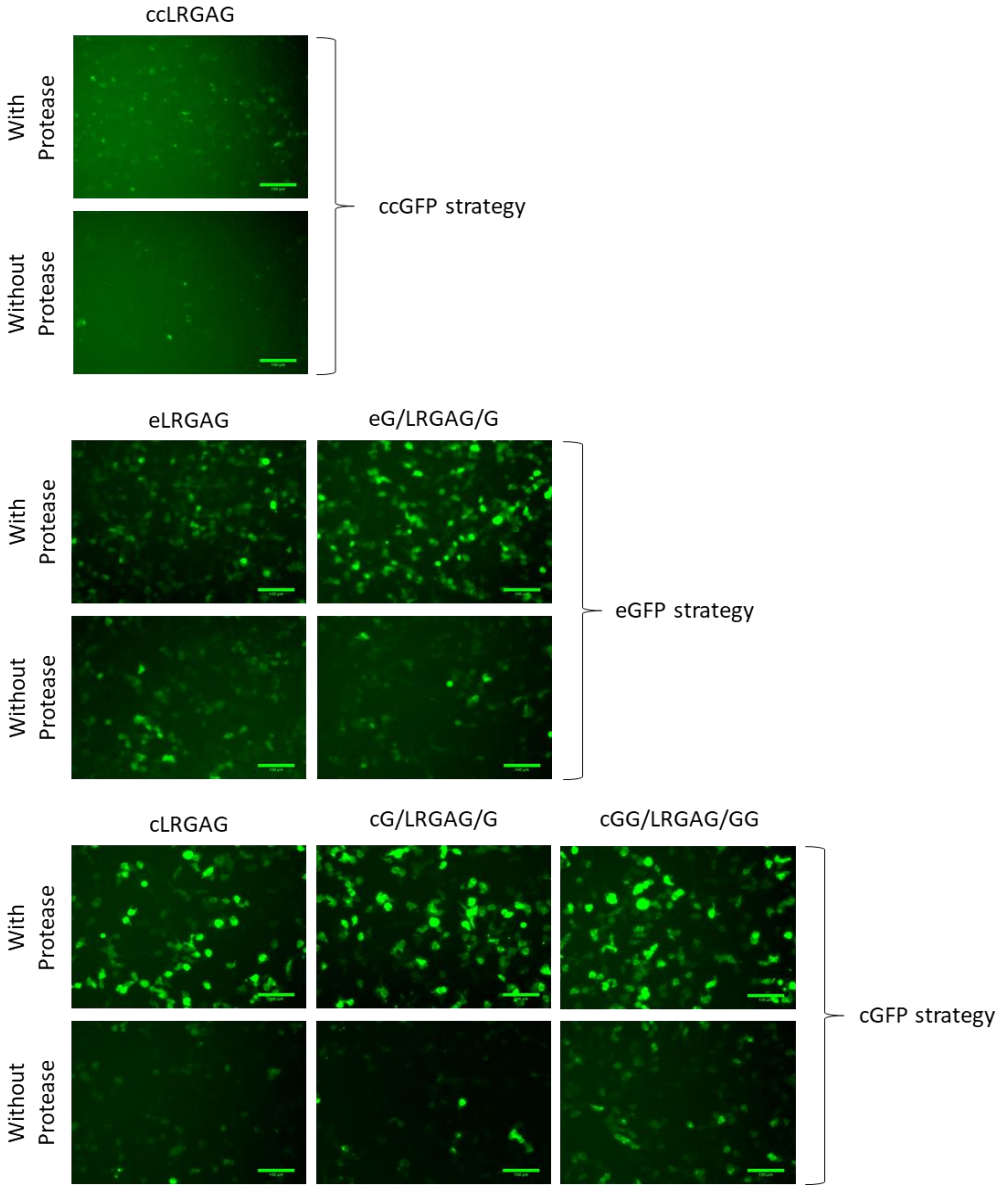

Figure 3.1: Fluorescence microscopy images of the adenoviral VISENSORS designed with different backbones. HEK 293T cells were transiently co-transfected with a protease or a mock plasmid (containing the fluorescent reporter mCherry), the GFPS10, and different GFPS11 containing different backbones. Forty-eight hours later, fluorescence emission was assessed by fluorescence microscopy. For the eGFP strategy, 2 GFPS11 backbones were evaluated: eLRGAG and eG/LRGAG/G. For the cGFP strategy, 3 GFPS11 backbones were tested; cLRGAG, cG/LRGAG/G and cGG/LRGAG/GG. Scale Bar: 100 µm.

Because different cleavable likers might induce different degrees of structural distortion and different cleavage efficiencies, their performance was evaluated in a transient screening. At total three different backbones were tested: LRGAG, was used in the design of the GFPS11 of all strategies tested. G/LRGAG/G – which has glycine spacers surrounding the cleavable sequence in order to increase its exposure to protein recognition - was employed in the design of the GFPS11 of the eGFP and cGFP strategies. Finally, the GG/LRGAG/GG backbone – with two glycine spacers surrounding the cleavable sequence - was only tested for the GFPS11 of the cGFP strategy.

For this initial characterization, HEK 293T cells were transiently co-transfected with each version of the sensor strategies with an adenoviral PR or a mock plasmid. As seen by fluorescence microscopy (**Figure 3.1**) co-transfection of each version of the sensors with the adenoviral PR led to an increase of GFP fluorescence emission when compared to co-transfection with the mock plasmid. It is also noticeable that the presence of the glycine spacers results in an increase of the GFP fluorescence emission either in the presence of PR or in its absence. When comparing strategies, the lowest GFP fluorescence emission was observed in ccGFP strategy; eGFP and cGFP seem to have similar GFP fluorescence emission.

Flow cytometry analysis showed that the ccGFP strategy reached a S/N ratio (2.1 ± 0.3) very similar to that of the eLRGAG (2.3±0.5) and eG/LRGAG/G (2.2±0.1) backbones used for the eGFP strategy. The cGFP strategy showed the highest S/N ratio peformance: cLRGAG (3.9±0.5), cG/LRGAG/G (4.0±0.3) and cGG/LRGAG/GG (2.7±0.1) (**Figure 3.2**).

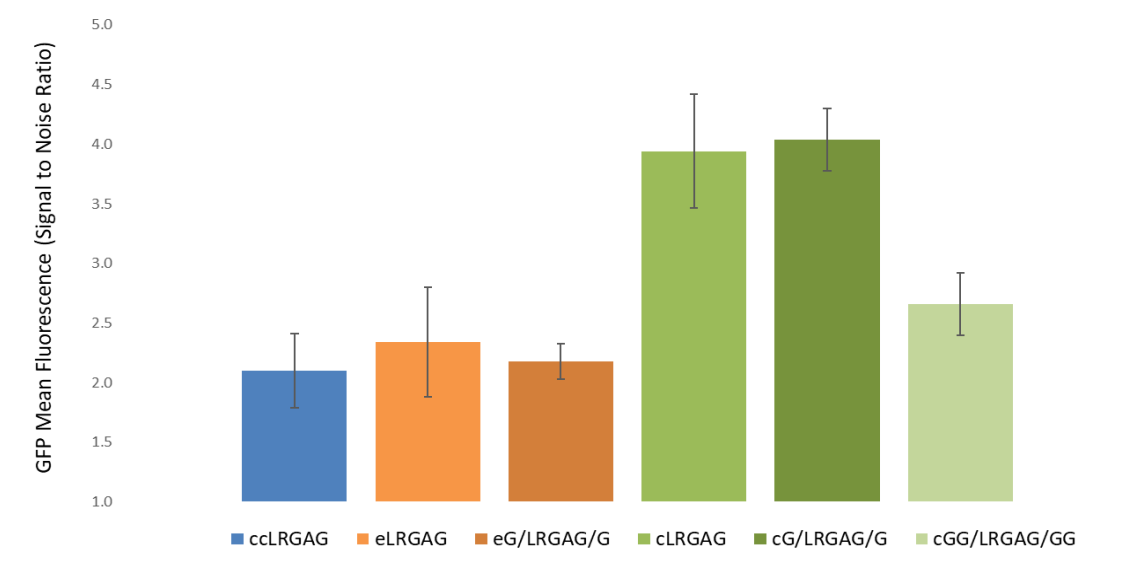

Figure 3.2: Adenoviral VISENSORS Signal/Noise ratios obtained for the different strategies and backbones. HEK 293T cells were transiently co-transfected with a PR or a mock plasmid (containing the fluorescent reporter mCherry), the GFPS10 and a different GFPS11 backbone. For the ccGFP strategy, the GFPS11 backbone tested was the ccLRGAG. For the eGFP strategy 2 backbones were evaluated: the eLRGAG and the eG/LRGAG/G. Finally, for the cGFP strategy 3 backbones were tested: cLRGAG, cG/LRGAG/G and cGG/LRGAG/GG. S/N ratio was determined based on flow cytometry data collected 48 hours after transfection. Results represent mean ± standard deviation of at least 3 independent experiments.

The backbone with the higher S/N ratio was selected in each strategy: eGFP and cGFP to undergo a stable screening.

For the establishment of a population stably expressing each sensor strategy, HEK 293 cells were transduced at a MOI of 5 with lentiviral vectors having as transgene the GFPS10; then cells were selected through zeocin. Afterwards, selected cells were transduced with lentiviral vectors containing the GFPS11 at a MOI of 5 and selected through puromycin. The eLRGAG and cG/LRGAG/G populations were previously constructed to this thesis work. For the ccGFP strategy we were unable to establish a stable population.

3.2. eGFP strategy for Adenoviral VISENSORS- eLRGAG backbone characterization by ADV5 infection

To evaluate the sensor response towards ADV5 infection, HEK 293 cell populations stably expressing the eLRGAG GFPS11 backbone were infected with a label-free ADV5 at a MOI of 5 in order to obtain a synchronised infection. As seen in **Figure 3.3**, the GFP fluorescence emission increased 24 hours after the infection, reaching its maximum intensity at 48 hours after infection. The S/N ratios present in **Figure 3.4** at 24 hours (1.4±0.1), 48 hours (2.01±0.09) or 72 hours (1.5±0.2) after infection are, however, smaller when compared to the ones obtained in transient (2.3±0.5) 48 hours after transfection (**Figure 3.3**).

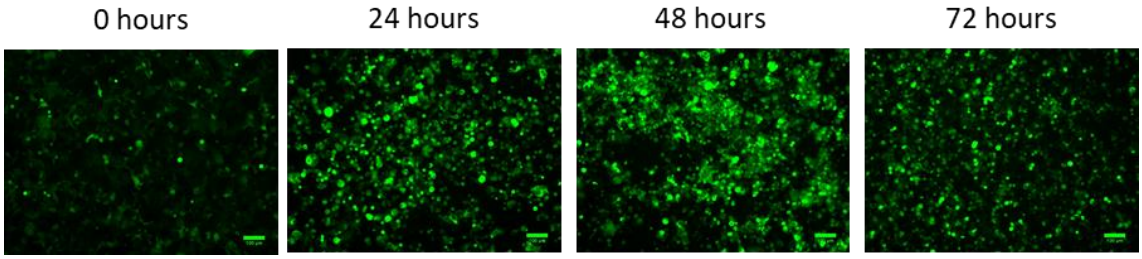

Figure 3.3: Adenoviral VISENSOR fluorescence microscopy images obtained for the eLRGAG backbone stably expressed in HEK 293 cells. HEK 293 cells stably expressing GFPS10 and the backbone eLRGAG for the GFPS11 were infected with ADV5 at a MOI of 5 and analysed by fluorescence microscopy at the given time points.
Scale Bar: 100 µm

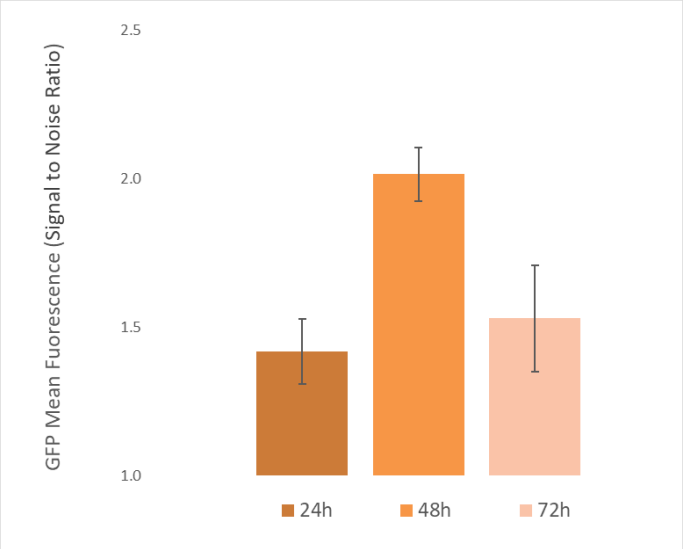

Figure 3.4: Adenoviral VISENSOR Signal/Noise ratios obtained for the eLRGAG backbone stably expressed in HEK 293 cells. HEK 293 cells stably expressing GFPS10 and the backbone eLRGAG for the GFPS11 were infected with ADV5 at a MOI of 5. At the given time post-infection, cells were analysed by flow cytometry with late apoptotic cells being excluded by propidium iodide. GFP mean fluorescence of live cells was measured for the S/N ratio calculations. Results represent mean ± standard deviation of 3 biologic replicates.

3.3. cGFP strategy for Adenoviral VISENSORS - cG/LRGAG/G cleavable characterization by ADV5 infection

To evaluate the sensor response towards ADV5 infection, HEK 293 cell populations stably expressing the cG/LRGAG/G GFPS11 backbone were infected with a label-free ADV5 at a MOI of 5. As shown in **Figure 3.5**, the GFP fluorescence emission after infection increases, but then tends to stabilize and overall is lower when compared to the eLRGAG populations tested in stable for the same periods of time.

The S/N ratios obtained for the 24 hours (1.2±0.5), 48 hours (1.6±0.1) and 72 hours (1.6±0.1) after infection are lower than the ones obtained in transient (2.2±0.2) (**Figure 3.6**).

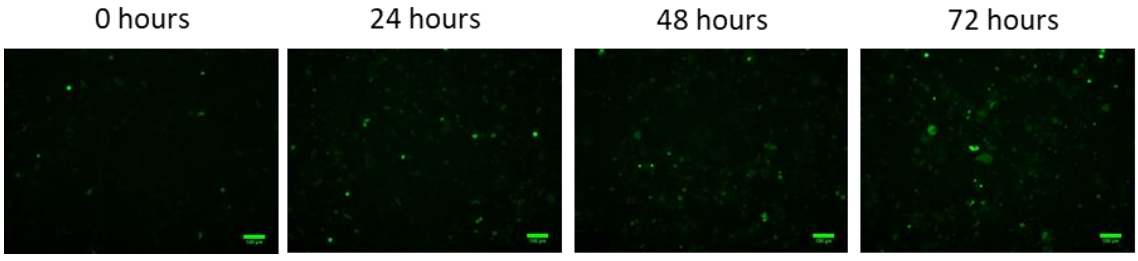

Figure 3.5: Adenoviral VISENSOR fluorescence microscopy images obtained for the cG/LRGAG/G backbone stably expressed in HEK 293 cells. HEK 293 cells stably expressing GFPS10 and the backbone cG/LRGAG/G for the GFPS11 were infected with ADV5 at a MOI of 5 and analysed by fluorescence microscopy at the given time points.
Scale Bar: 100 µm

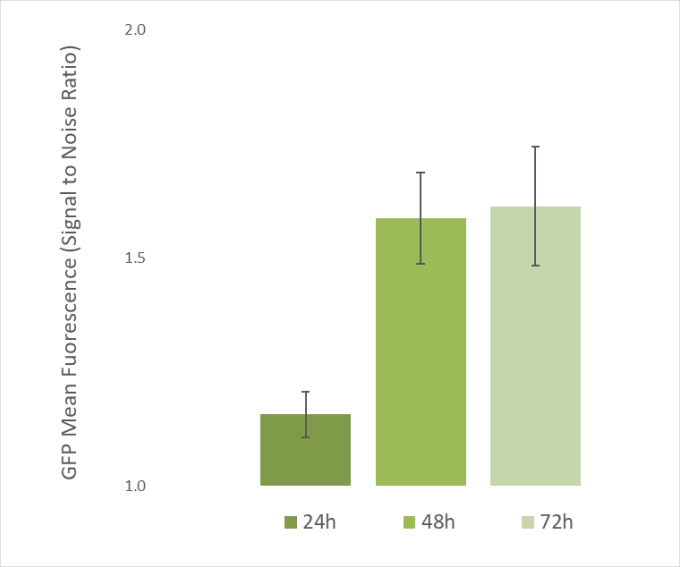

Figure 3.6: Adenoviral VISENSOR Signal/Noise ratios obtained for the cG/LRGAG/G backbone stably expressed in HEK 293 cells. HEK 293 cells stably expressing GFPS10 and the backbone cLRGAG for the GFPS11 were infected with ADV5 at a MOI of 5. At the given time post-infection, cells were analysed by flow cytometry with late apoptotic cells being excluded by propidium iodide. GFP mean fluorescence of live cells was measured for the S/N ratio calculations. Results represent mean ± standard deviation of 3 biologic replicates.

3.4. Characterisation of the eGFP and cGFP VISENSORS

Because of the discrepancies verified between the S/N ratios obtained in the transient and stable screenings, through characterization of eGFP and cGFP VISENSORS was performed.

The eGFP and cGFP populations were developed on top of the same GFPS10 parental population. Therefore, to evaluate if the VISENSORS had sufficient (and similar) GFPS10 levels, the eGFP and the cGFP cell populations, as well as a control GFPS10 parental population, were infected with retroviral virus at a MOI of two possessing as transgene a LacZ-GFPS11, were the GFPS11 was not distorted. Since the GFPS11 present in the retroviral virus did not have a structural distortion, unlike the GFPS11 already present in the eGFP and cGFP cell populations, it is available to transcomplement with the GFPS10 present in either one of these three cell populations.

Figure 3.7 illustrates the flow cytometry data concerning these three cell populations. Since cells were infected with a MOI of 2, a synchronized infection was not achieved and as expected the flow cytometry data of the infected samples shows two green peaks, with the right peak illustrating the cells infected where GFP fluorescence intensity is higher. When compared, all three populations reached similar values of GFP fluorescence intensity in the presence of the retroviral virus: 26±3 31±5 and 29±2 for GFPS10, eGFP and cGFP populations, respectively (**Figure 3.8 A**). This result suggested that eGFP and cGFP populations had similar levels of GFPS10 available for transcomplementation with GFPS11.

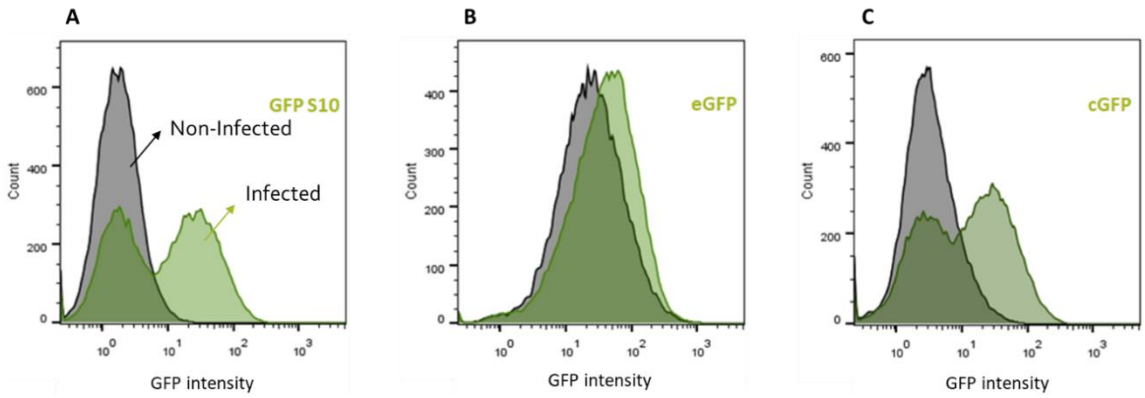

Figure 3.7: HEK 293 cell populations stably expressing the GFPS10, eGFP or cGFP infected with retroviral virus containing the GFPS11 non-distorted. Flow cytometry analysis of HEK 293 cells acquired 48 hours after infection with retroviral virus at a MOI of 2 having as transgene the LacZ-GFPS11. Non-infected cells appear in grey and the infected are showed in green. **(A)** HEK 293 cell population stably expressing the GFPS10 (parental cell population that was afterwards transduced with the GFPS11 backbone for either the eGFP or cGFP strategies); **(B)** HEK 293 cell population stably expressing eGFP strategy with the eLRGAG GFPS11 backbone; and **(C)** HEK 293 cell population stably expressing cGFP strategy with the cG/LRGAG/G GFPS11 backbone.

Regarding S/N performance, GFPS10 when transcomplemented with LacZ-GFPS11 represents the maximum S/N that could be achieved by any strategy system (22±3) (**Figure 3.8 B**). The maximal S/N performance of the VISENSORS populations are, however, lower, with eGFP and cGFP showing a maximal S/N of 1.3±0.2 and 13±1, respectively. Despite, VISENSORS populations attain similar GFP mean fluorescence values upon ADV5 infection, their potential as sensors is lower due to higher background fluorescence especially the eGFP strategy where the Noise is almost the same as the Signal.

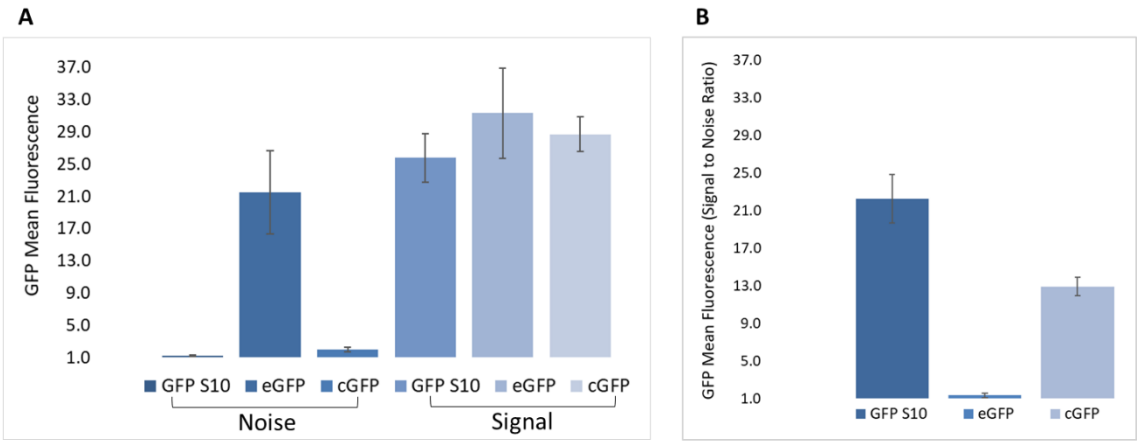

Figure 3.8: Values of GFP mean fluorescence Signal and Noise acquired after HEK 293 cell populations stably expressing the GFPS10, eGFP or cGFP were infected with retroviral virus containing LacZ-GFPS11 non-distorted and respective Signal/Noise ratios. HEK 293 cell populations expressing the GFPS10, eGFP or cGFP were infected with retroviral virus at a MOI of 2 containing the lacZ-GFPS11 as transgene, where the GFPS11 is not distorted. Forty-eight hours after infection cells of 3 biological replicates were analysed by flow cytometry where **(A)** the GFP mean fluorescence was assessed and **(B)** S/N ratios were calculated. Results represent mean ± standard deviation of 3 biological replicates.

To assess if the differences verified between transient and in stable were caused by a lack of GFPS11 (VISENSORS) stable expression in the HEK 293 cells, a qPCR was conducted.

Since development of the VISENSORS stable cell populations were obtained through transduction with lentiviral vectors, a qPCR was performed to detect transgene integrated copy numbers using primers specific for the LTR and WPRE. As the parental GFPS10 population already has the LTR and WPRE integrated, for the integration analysis of the VISENSORS a relative quantification was conducted, normalized towards the ribosomal protein L22 (RPL22) and compared with the parental GFPS10 population, applying the $2^{-\Delta\Delta Cp}$ method (Livak and Schmittgen, 2001).

As showed in **Figure 3.9**, eGFP (2.35±0.08; 2.3±0.4, for LTR and WPRE, respectively) and cGFP (1.93±0.06; 2.06±0.08, for LTR and WPRE, respectively) populations have similar levels of integrated copies of GFPS11.

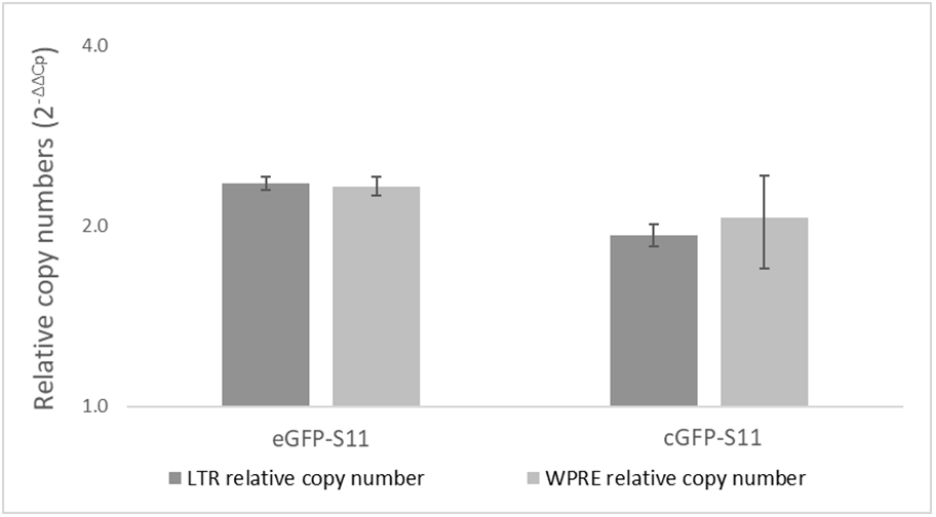

Figure 3.9: Relative GFPS11 copy numbers integrated in eGFP and cGFP VISENSOR cell populations. The LTR and WPRE relative copy numbers of HEK 293 cells stably expressing the eGFP or cGFP was normalised towards the ribosomal protein L22 (RPL22) and compared with the GFPS10 parental population using the $2^{-\Delta\Delta Cp}$ method. Results represent mean ± standard deviation of 2 independent experiments.

3.5. HIV-1 Protease assessment under transient expression in HEK 293T cells

Since the use of lentiviral vectors in gene therapy clinical trials is increasing, the VISENSORS were adapted to the HIV-1 PR. For its performance evaluation in a transient manner a HIV-1 PR was constructed based on Konvalinka et al work (Konvalinka *et al.*, 2001) to try to produce a PR highly expressed. To this end, the PR needs to be produced as a fusion protein, containing the cleavage sites for its autoproteolysis and for its activation the first amino acid needs to be a proline.

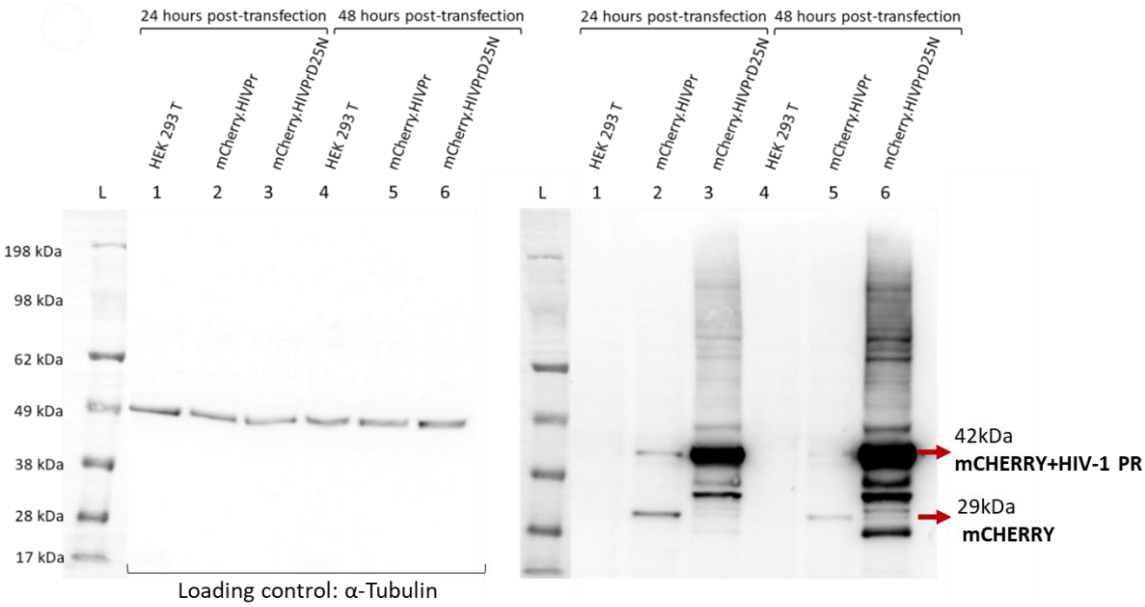

Figure 3.10: HIV-1 PR activity assessment. Western blotting analysis of HEK 293T cell extracts transfected with the active or inactive HIV-1 PR fused to an mCherry were analysed by immunoblotting. Anti-mCherry and anti-α-Tubulin (loading control) primary antibodies were used.

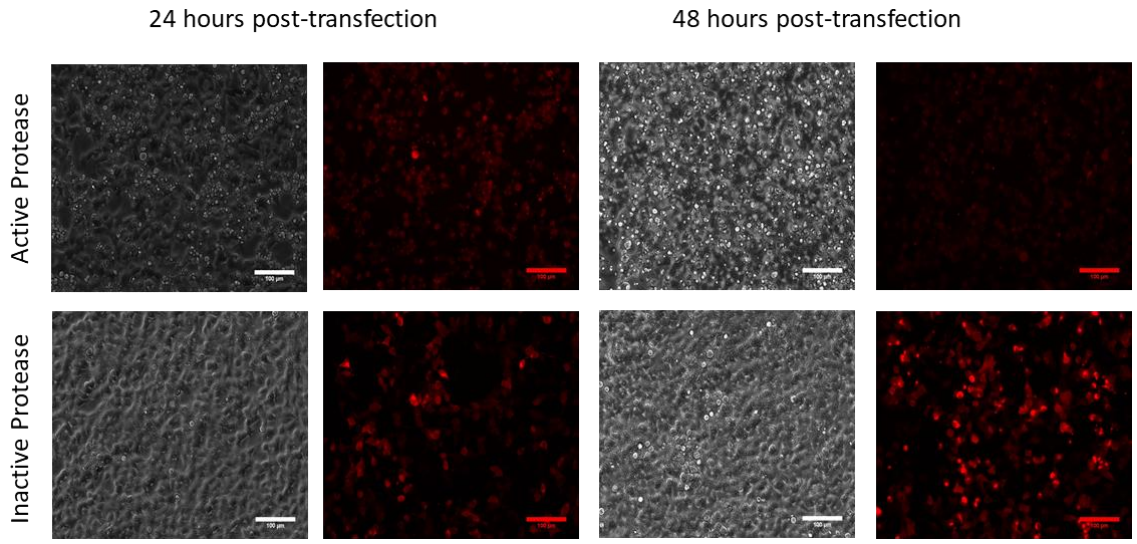

Figure 3.11: Fluorescence microscopy images of HEK 293T cells transfected with the active or inactive form of HIV-1 Protease. HEK 293T cells were transfected with the active HIV-1 protease fused to an mCherry or with the inactive HIV-1 protease (D25N mutation) fused to mCherry.
Scale bar: 100 µm

To confirm the HIV-1 PR activity, protein extracts from cells transfected with the active or inactive HIV-1 PR fused to mCherry were analysed by Western blotting (**Figure 3.10**).

As shown in lanes 2 and 5, active HIV-1 PR is able to excise itself from the fusion protein, resulting in the detection of a 32 kDa mCherry protein. The inactive version (lanes 3 and 6) is not able to excise itself, resulting in the detection of the fusion protein mCherryHIV-1PRD25N

with approximately 42 kDa. However, unspecific bands are visible in lanes 2, 3, 5 and 6 might be due to mCherry isoforms or more likely result from protein degradation.

Phase contrast and fluorescence microscopy of cells transiently transfected with these constructs (**Figure 3.11**) showed evident cell death when in the presence of the active PR but not in the presence of the inactive PR. Indeed, mCherry fluorescence emission is lower in the presence of the active PR, corroborating the induction of cell death.

Therefore and since this construct induces extensive cell death, for transient screenings of HIV-1 VISENSORS we made use of pMDLg/pRRE plasmid coding HIV-1 PR, leading to a lower expression level of the protease with no visible cell death,

3.6. Backbones performance analysis for HIV-1 VISENSORS in transient screening

For the development of a fluorescent cell-based biosensor for detection of label-free lentiviruses, the GFPS11 of the eGFP and cGFP strategies was modified to contain an HIV-1 cleavage sequence. A total of three backbones were constructed to be tested in these two strategies: GIF↓LET, GSGIF↓LETSL and IRKIL↓FLDG.

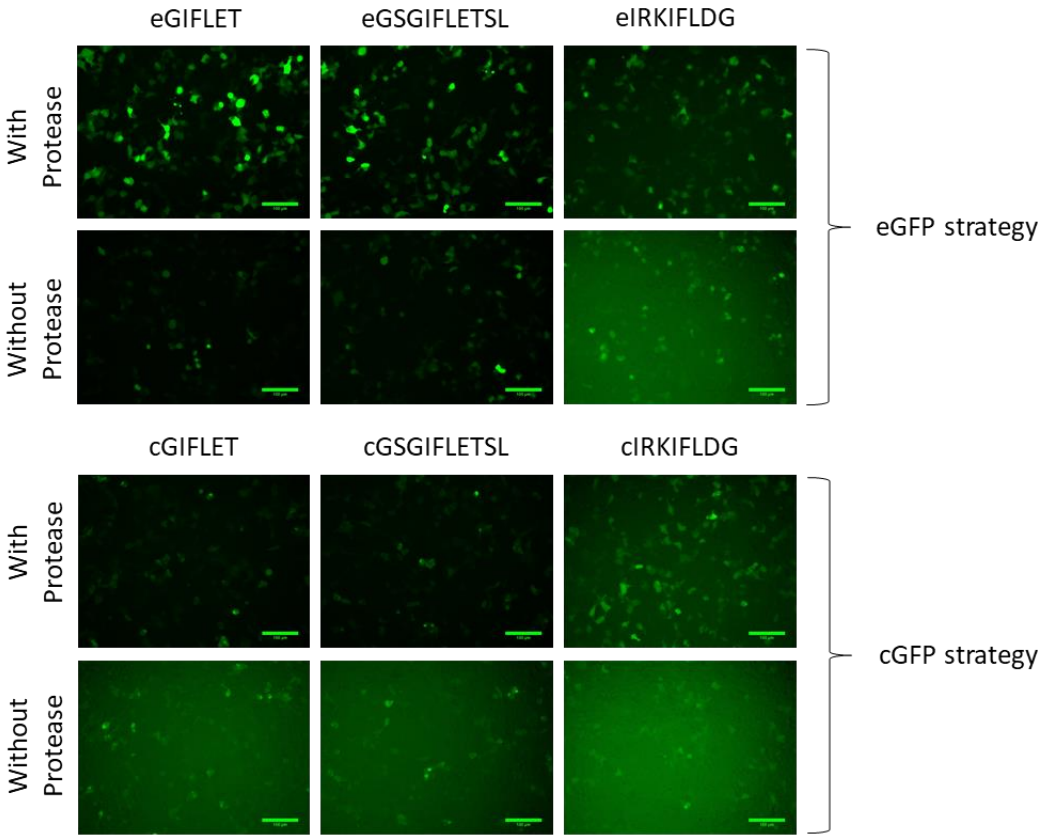

Figure 3.12: HIV-1 VISENSORS fluorescence microscopy images obtained for the different backbones and cleavable sequences. HEK 293T cells were transiently co-transfected with a Protease or a mock plasmid (containing the fluorescent reporter mCherry), the GFPS10, and a different GFPS11 backbone. Forty-eight hours after transfection, fluorescence emission was assessed by fluorescence microscopy.

Scale bar: 100 µm

To evaluate the different backbones and cleavable sequences tested within each strategy a transient screening was performed, were HEK 293T cells were transiently co-transfected with each version of the sensor strategies and with an HIV-1 PR or a mock plasmid. As seen by fluorescence microscopy (**Figure 3.12**) the GFP fluorescence emission increases in the presence of the viral PR, suggesting successful adaptation and functionality of the HIV-1 VISENSORS to respond to HIV-1 protease activity. In addition, the IRKILFLDG backbone showed the lowest GFP fluorescence emission in either one of the strategies tested; the GFP fluorescence emission of the GIFLET and GSGIFLET are similar within each strategy.

Flow cytometry results (**Figure 3.13**) showed that the IRKILFLDG exhibit the lowest S/N ratios for the eGFP (2.7±0.2) or cGFP (2.5±0.3) strategies. The S/N ratios for the eGIFLET(3.0±0.4) and eGSGIFLETSL (3.1±0.4) are similar to those obtained for the cGIFLET (3.0±0.5) and cGSGIFLETSL (3.1±0.6) backbones.

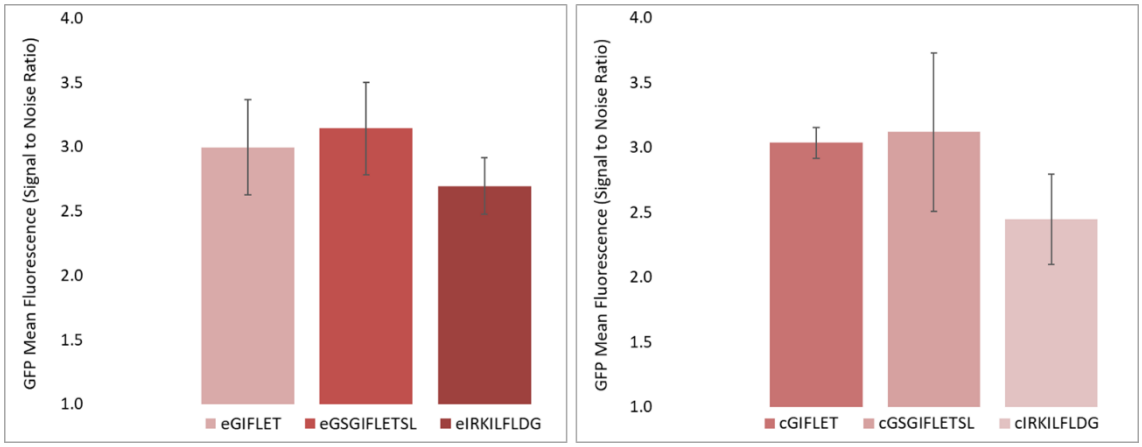

Figure 3.13: HIV-1 VISENSORS Signal/Noise ratios obtained for the different backbones tested using the different strategies. HEK 293T cells were transiently co-transfected with a PR or a mock plasmid (containing the fluorescent reporter mCherry), the GFPS10, and a different GFPS11 backbone. Results represent mean ± standard deviation of at least 3 independent experiments.

4. Discussion and conclusions

VBBs are part of a segment in the pharma industry where the recent investment is resulting in the production of new therapies, such as the novel vectored vaccines. For vaccines development is necessary to access the vaccine's efficiency and for this, virus titration is imperative. The field of gene therapy has also experienced a substantial growth. The number of clinical trials is currently increasing and, consequently, numerous products are reaching the market in the last years. Viral vectors are VBBs and remain the approach most used for gene delivery due to their efficiency. As so, a high-throughput and fast method for quantification of viral vectors is needed to know the amount of viral vectors that should be administrated per target cell.

However, present titration methods are time consuming and fail to provide a reliable and robust quantification of infectious particles. Additionally, some of them require the use of a reporter gene, which implicates the modification of the viruses that cannot be used for clinical purposes due to their immunogenicity risks (Ansari *et al.*, 2016). Therefore, robust and standardized methods of titration are needed.

In this context, this thesis aimed to develop a fluorescent cell-based sensor for detection and quantification of viral vectors. The sensors were developed for label-free viruses eliminating the safety concerns that the reporters carry. Since adenoviral vectors remain the most used for gene therapy clinical trials (**Figure 1.3**), the design of the first sensor was focused on these viral vectors and three strategies were tested: ccGFP, eGFP and cGFP.

As a proof of concept, the performance of several backbones was evaluated in a transient manner through fluorescence microscopy and flow cytometry (**Figures 3.1 and 3.2**). The results obtained showed that the sensors are activated by the PR, since in its presence the GFP fluorescence emission increases. The addition of glycines surrounding the cleavable sequence led to an increase of the GFP fluorescence emission. This might be due to a more exposed cleavable sequence, by inducing a more flexible conformation in this area of the molecule, therefore increasing the cleavage efficiency by the PR. However, the GFP background fluorescence emission – when no protease is added – also increased. This suggests then a reduction in the structural distortion of the GFPS11.

The two most promising strategies - eGFP and cGFP - were tested in stable cell populations - HEK 293 cells stably expressing VISENSORS - to mimic the biological context of the ADV5 infection, which is the final design for sensor application purposes. In these conditions, the eGFP strategy with the GFPS11 eLRGAG backbone shows that is functional because its GFP fluorescence increases in the presence of the viral PR, reaching its highest S/N ratio at 48 hours after infection with label-free ADV5 (**Figures 3.3 and 3.4**). After this time point, a reduction in fluorescence emission is observed. This might be due to the lytic nature of the ADV5. where the majority of cells are experiencing cell death. Even though we used propidium iodide (PI) to exclude cells in late apoptosis. GFP fluorescence of cells in early apoptosis

although lower - cessation of gene expression and sensor degradation – is taken into account when calculating S/N performance.

The S/N ratios obtained in stable conditions for either one of the backbones sensors - eLRGAG (2.01±0.09) and cG/LRGAG/G (1.6±0.1) - were lower than the ones achieved in transient - eLRGAG (2.3±0.5) and cG/LRGAG/G (4.0±0.3). This might be explained by the high levels of protein expression obtained on transient transfections that are not obtained in stable expression, making these two conditions not directly comparable.

For both sensors' strategies eGFP and cGFP in stable the S/N was detected at 24 hours after infection which is coincident with the virus life cycle, since the ADV5 PR only starts to be expressed 18 hours after infection. Also, for both sensors' strategies in stable the S/N ratio increases from the 24 hours to the 48 hours after infection, this might be explained by an higher PR concentration in the cell, due to the replication cycle of the virus and so, the novel PRs will contribute to increase the S/N ratio. So, we can conclude that for the maximum S/N ratio (48 hours after infection) be attained, the sensor should be applied to replicative virus, that can generate more PRs to amplify the Signal in order to be robustly detected.

The cGFP strategy in transient reached a S/N ratio that was 2.0 times superior than the obtained for the eGFP strategy; however, in stable the S/N ratio of the eGFP was only 1.3 times higher than the attained for the cGFP strategy. In order to understand better the cause for these discrepancies between transient and stable conditions and, more importantly, why cGFP strategy in stable shows low S/N ratio performance, GFPS10 and GFPS11 levels were assessed.

To evaluate if GFPS10 expression levels were limiting sensor performance, the eGFP and cGFP cell populations, as well as the GFPS10 parental population were compared. Upon infection with retroviral viruses harbouring LacZ-GFPS11 (with no structural distortion), the parental GFPS10 population reached the maximum fluorescence emission that is possible to attain, GFPS11 is readily available (no PR needed) resulting in a theoretical maximal S/N ratio performance of 22±3. Since the VISENSORS strategies eGFP and cGFP were developed on top of this GFPS10 parental population, it was expected that they could share the same S/N potential. However, both showed lower performances - 1.3±0.2 and 13±1, respectively. This can be explained by the high background fluorescence emission, suggesting that distortion of GFPS11, especially when embedded in Eglin c protein loop, is not enough to prevent transcomplementation in absence of the viral PR.

Since the GFP fluorescence emission of the three populations after infection with the LacZ-GFPS11 is similar (**Figure 3.8 A**), it suggested that sensor populations, eGFP and cGFP, have similar levels of GFPS10 expression. Therefore, lower S/N performance of cGFP is not explained by a lack of GFPS10 available for transcomplementation after sensor activation by the adenoviral PR.

cGFP strategy has the potential to attain a S/N ratio of 13±1 (**Figure 3.8 B**), but its only achieving a S/N of 1.6±0.1 (**Figure 3.6**) when infected with ADV5. This might be caused by: a) low levels of GFPS11 expression; b) GFPS11 being inefficiently cleaved; or c) GFPS11 might

be degraded. Therefore, to determine if the GFPS11 levels were limiting sensor performance, GFPS11 expression levels were assessed. The lack of antibodies against the small peptide GFPS11 impaired the use of Western blotting technique to assess GFPS11 protein expression. Therefore, we performed a qPCR to search for integrated viral DNA. Since GFPS11 were delivered through lentiviral transduction, and since lentiviruses have an integration pattern preferring DNA regions with high levels of gene expression, it was assumed that, given the same amount of integrated copies of GFPS11 - eLRGAG and cG/LRGAG/G - these have similar expression levels. The $2^{-\Delta\Delta Cp}$ method (Livak and Schmittgen, 2001) was used to normalize the integrated LTR and WPRE relative copy numbers of the eGFP and cGFP VISENSORS population towards the GFPS10 parental population LTR and WPRE copy numbers (**Figure 3.9**). Both populations - eGFP and cGFP - seem to have similar quantities of GFPS11 integrated into their genomes due to similar integrated LTR and WPRE relative copy numbers. Even though the LTR and WPRE relative copy numbers of the eGFP population are a little higher than those obtained for the population with the cGFP sensor, this difference is not enough to explain the higher background fluorescence emission obtained with this strategy.

All in all, these results suggest that the cGFP strategy, with similar levels of GFPS10 and GFPS11 to the eGFP strategy, does not achieve its maximal S/N potential 13±1 (**Figure 3.8 B**) due to unidentified effects, such as early protein degradation, low transcomplementation efficiency when stably expressed (lower protein expression levels compared to transient transfection), or others, needing further investigation.

In conclusion, three different strategies were developed - ccGFP, eGFP and cGFP – all able to detect the ADV5 PR activity in transient conditions. As for stable conditions, the eGFP strategy showed to be the most promising, but its high background fluorescence emission (when no PR is present) impacts its S/N performance. Further work is needed to increase the structural distortion of this sensor, such as for example remove amino acids or by adding a tag for degradation of the GFPS11.

The usage of lentiviral vectors in gene therapy clinical trials, particularly those derived from HIV-1, has been increasing due to their lower immunogenicity, ability to transduce non-dividing cells and permanently modify cells (Naldini *et al.*, 1996). Therefore, the above validated VISENSORS for detection of adenovirus PR activity, were adapted for detection of HIV-1 PR activity by substitution and optimization of the specific cleavage sequences.

First and to test functionality of these VISENSORS, a plasmid encoding the HIV-1 PR was constructed to be used for the HIV-1 VISENSORS transient screening. To improve HIV-1 PR expression and activity, this PR was fused to an mCherry to prevent protein precipitation (Konvalinka *et al.*, 2001), and express an active PR. Western blotting analysis of extracts of transfected HEK 293T cells (**Figure 3.10**) confirmed that the fusion protein mCherry-HIV-1 PR was indeed active, as seen by the detection of mCherry protein alone (HIV-1 cleaves itself from the fusion protein). However, these HEK 293T cells transfected with the active form of the HIV-1 PR exhibited extensive cell death **(Figure 3.11)** due to the cytotoxicity of the protease (Konvalinka *et al.*, 2001; Nguyen *et al.*, 2015). As expected, this effect is not observed when

cells are transfected with the inactive version of the PR. The cytotoxicity induced by the active HIV-1 PR is also corroborated by the decrease of the mCherry fluorescence, caused by the reduction in expression of this protein, a consequence of cell death.

Due to the cytotoxic effect, this PR version could not be used to perform the transient screening of the HIV-1 VISENSORS. Instead, a less cytotoxic version of HIV-1 PR was used. The pMDLg/pRRE plasmid encodes the Gag-Pro-Pol sequence, where for 20 Gag proteins that are translated only 1 PR is translated (Hoggard and Owen, 2003).

For the HIV-1 VISENSORS the eGFP and cGFP strategies were adapted to contain HIV-1 cleavable sequences. For both strategies, three different cleavable sequences - GIFLET, GSGIFLETSL and IRKILFLDG - were tested in transient transfections (**Figures 3.12 and 3.13**). The results showed that, for all cleavable sequences tested, the sensors are indeed being activated as seen by the increase in GFP fluorescence emission when HIV-1 PR is added.

Cleavable sequence IRKILFLDG exhibited the lowest S/N ratios and fluorescence emissions. This might be due to the hydrophobicity of the majority of the amino acids present in the cleavable sequence, which can reduce solvent exposure and consequently lead to a less effective cleavage. The GIFLET and GSGIFLETSL backbones showed similar results; however, the GSGIFLETSL backbone attained slightly higher S/N ratios in both strategies. As future work their performance should be further evaluated by conducting a screening in stable cell populations in response to viral infection.

During this thesis, cell populations stably expressing VISENSORS were analysed. As such, S/N performance is averaged. Since different ratios of GFPS10 and GFPS11 might impact sensor performance, a screening of several cell clones stably expressing the ADV5 or HIV-1 VISENSORS should be additionally performed aiming at finding those clones with the best S/N performances. The selected clones should be further analysed in terms of the sensor activation kinetics, optimal time point of analysis after infection, and their applicability as a quantification method through the construction of a calibration curve using different MOIs.

All in all, this work contributed for the optimization of cell-based fluorescent biosensors able to detect specific viral PR activity, either from ADV or HIV-1. The ADV5 VISENSORS have showed their applicability to detect label-free virus's infection and were further characterized in terms of their limitations, resulting in some enlightenment on the possible improvements that should be made in order to accomplish a stronger detection signal. The strategies here explored have the potential to be implemented in the detection of other label free replicative viruses, by simple modification of the specific cleavable sequence.

VISENSORS provide a fast and reliable method for detecting PR activity in mammalian cells and have the potential to be used as a high-throughput system when coupled with a fluorometer plate reader for detection and quantification of viruses and viral vectors, with numerous applications in the fields of gene therapy, vaccine development, and antiretroviral drugs research.

5. References

Al-Dosari, M. S. and Gao, X. (2009) 'Nonviral Gene Delivery: Principle, Limitations, and Recent Progress', *The AAPS Journal*, 11(4), pp. 671–681. doi: 10.1208/s12248-009-9143-y.

Ansari, A. M. *et al.* (2016) 'Cellular GFP Toxicity and Immunogenicity: Potential Confounders in in Vivo Cell Tracking Experiments', *Stem Cell Reviews and Reports*. Stem Cell Reviews and Reports, 12(5), pp. 553–559. doi: 10.1007/s12015-016-9670-8.

Arthur, L. O. *et al.* (1992) 'Cellular proteins bound to immunodeficiency viruses: implications for pathogenesis and vaccines.', *Science (New York, N.Y.)*, 258(5090), pp. 1935–8. doi: 10.1126/science.1470916.

Beck, Z. Q. *et al.* (2000) 'Identification of efficiently cleaved substrates for HIV-1 protease using a phage display library and use in inhibitor development', *Virology*, 274(2), pp. 391–401. doi: 10.1006/viro.2000.0420.

Bergelson J. A. Cunningham, G. Droguett, E. A. Kurt-Jones, A. Krithivas, J. S. Hong, M. S. Horwitz, R. L. Crowell and R. W. Finberg., J. M. (1997) ' Isolation of a common receptor\rfor Coxsackie B viruses and adenoviruses 2 and 5.', *Science*, 275, pp. 1320–1323.

Callahan, B. P., Stanger, M. J. and Belfort, M. (2010) 'Cut and glow: Protease activation of split green fluorescent protein', *Chembiochem : a European journal of chemical biology*, 11(16), pp. 2259–2263. doi: 10.1002/cbic.201000453.

Callahan, B. P., Stanger, M. J. and Belfort, M. (2010) 'Protease Activation of Split Green Fluorescent Protein', *ChemBioChem*, 11(16), pp. 2259–2263. doi: 10.1002/cbic.201000453.

Chalfie, M. *et al.* (1994) 'Green fluorescent protein as a marker for gene expression', *Science*, 263(5148), pp. 802–805. doi: 10.1126/science.8303295.

Chen, P. H., Ornelles, D. A. and Shenk, T. (1993) 'The adenovirus L3 23-kilodalton proteinase cleaves the amino-terminal head domain from cytokeratin 18 and disrupts the cytokeratin network of HeLa cells.', *Journal of virology*, 67(6), pp. 3507–14.

Chou, K. C. (1996) 'Prediction of human immunodeficiency virus protease cleavage sites in proteins.', *Analytical biochemistry*, 233(1), pp. 1–14. doi: 10.1006/abio.1996.0001.

Coffin, J. (1995) 'HIV population dynamics in vivo: implications for genetic variation, pathogenesis, and therapy', *Science*, 267(5197), pp. 483–489. doi: 10.1126/science.7824947.

Cotten, M. and Weber, J. M. (1995) 'The adenovirus protease is required for virus entry into host cells', *Virology*, 213(2), pp. 494–502. doi: 10.1006/viro.1995.0022.

Courtenay, E. S. *et al.* (2000) 'Structural stability of binding sites: Consequences for binding affinity and allosteric effects', *Proteins: Structure, Function and Genetics*, 41(SUPPL. 4), pp. 63–71. doi: 10.1002/1097-0134(2000)41:4+<63::AID-PROT60>3.0.CO;2-6.

Damborsky, P., vitel, J. and Katrlik, J. (2016) 'Optical biosensors', *Essays In Biochemistry*, 60(1), pp. 91–100. doi: 10.1042/EBC20150010.

Devaux, C. *et al.* (1987) 'Crystallization, enzymatic cleavage, and the polarity of the adenovirus type 2 fiber', *Virology*, 161(1), pp. 121–128. doi: 10.1016/0042-6822(87)90177-2.

Ding, J. *et al.* (1996) 'Crystal structure of the human adenovirus proteinase with its 11 amino acid cofactor.', *The EMBO journal*, 15(8), pp. 1778–83. doi: 10.1002/j.1460-2075.1996.tb00526.x.

Diouri, M. *et al.* (1996) 'Cleavage efficiency by adenovirus protease is site-dependent', *Journal of Biological Chemistry*, 271(51), pp. 32511–32514. doi: 10.1074/jbc.271.51.32511.

Douglas, J. T. (2007) 'Adenoviral vectors for gene therapy', *Molecular Biotechnology*, 36(1), pp. 71–80. doi: 10.1007/s12033-007-0021-5.

Le Doux, J. M. *et al.* (1996) 'Proteoglycans secreted by packaging cell lines inhibit retrovirus infection.', *Journal of virology*, 70(9), pp. 6468–73.

Dull, T. *et al.* (1998) 'A third-generation lentivirus vector with a conditional packaging system.', *Journal of virology*, 72(11), pp. 8463–71. doi: 98440501.

Edwards, K. A. and Baeumner, A. J. (2006) 'Analysis of liposomes', *Talanta*, 68(5), pp. 1432–1441. doi: 10.1016/j.talanta.2005.08.031.

Ehreth, J. (2003) 'The value of vaccination: A global perspective', *Vaccine*, 21(27–30), pp. 4105–4117. doi: 10.1016/S0264-410X(03)00377-3.

Elsanhoury, A. *et al.* (2017) 'Accelerating Patients' Access to Advanced Therapies in the EU', *Molecular Therapy - Methods and Clinical Development*, 7, pp. 15–19. doi: 10.1016/j.omtm.2017.08.005.

Foldvari, M. *et al.* (2016) 'Non-viral gene therapy: Gains and challenges of non-invasive administration methods', *Journal of Controlled Release*, 240, pp. 165–190. doi:10.1016/j.jconrel.2015.12.012.

Frankel, A. D. and Young, J. A. T. (1998) 'HIV-1: Fifteen Proteins and an RNA', *Annual Review of Biochemistry*, 67(1), pp. 1–25. doi: 10.1146/annurev.biochem.67.1.1.

Fraser, M. J. and Hink, W. F. (1982) 'The isolation and characterization of the MP and FP plaque variants of Galleria mellonella nuclear polyhedrosis virus', *Virology*, 117(2), pp. 366–378. doi: 10.1016/0042-6822(82)90476-7.

Fritzsche, M. and Mandenius, C. F. (2010) 'Fluorescent cell-based sensing approaches for toxicity testing', *Analytical and Bioanalytical Chemistry*, 398(1), pp. 181–191. doi: 10.1007/s00216-010-3651-6.

Gates, I. V. *et al.* (2009) 'Quantitative measurement of varicella-zoster virus infection by semiautomated flow cytometry', *Applied and Environmental Microbiology*, 75(7), pp. 2027–2036. doi: 10.1128/AEM.02006-08.

Geraerts, M. *et al.* (2006) 'Comparison of lentiviral vector titration methods', *BMC Biotechnology*, 6, pp. 1–10. doi: 10.1186/1472-6750-6-34.

Ginn, S. L. *et al.* (2018) 'Gene Therapy Clinical Trials Worldwide To 2017 - an Update', *The Journal of Gene Medicine*, p. e3015. doi: 10.1002/jgm.3015.

Giriat, I. and Muir, T. W. (2003) 'Protein Semi-Synthesis in Living Cells', *Journal of the American Chemical Society*, 125(24), pp. 7180–7181. doi: 10.1021/ja034736i.

Greber, U. F. *et al.* (1996) 'The role of the adenovirus protease on virus entry into cells.', *The EMBO journal*, 15(8), pp. 1766–1777. doi: 10.1002/j.1460-2075.1996.tb00525.x.

Gueret, V. *et al.* (2002) 'Rapid titration of adenoviral infectivity by flow cytometry in batch culture of infected HEK293 cells', *Cytotechnology*, 38(1–3), pp. 87–97. doi: 10.1023/A:1021106116887.

Haramoto, E. *et al.* (2007) 'Recovery of naked viral genomes in water by virus concentration methods', *Journal of Virological Methods*, 142(1–2), pp. 169–173. doi: 10.1016/j.jviromet.2007.01.024.

Heim, R. and Tsien, R. Y. (1996) 'Engineering green fluorescent protein for improved brightness, longer wavelengths and fluorescence resonance energy transfer', *Current Biology*, 6(2), pp. 178–182. doi: 10.1016/S0960-9822(02)00450-5.

Henderson, L. E. *et al.* (1992) 'Gag proteins of the highly replicative MN strain of human immunodeficiency virus type 1: posttranslational modifications, proteolytic processings, and complete amino acid sequences.', *Journal of virology*, 66(4), pp. 1856–65.

Hoggard, P. G. and Owen, A. (2003) 'The mechanisms that control intracellular penetration of the HIV protease inhibitors', *Journal of Antimicrobial Chemotherapy*, 51(3), pp. 493–496. doi: 10.1093/jac/dkg137.

Höner, B., L Shoeman, R. and Traub, P. (1992) *Human immunodeficiency virus type 1 protease microinjected into cultured human skin fibroblasts cleaves vimentin and affects cytoskeletal and nuclear architecture*, *Journal of cell science*.

Huang, L., Li, Y. and Chen, C. (2011) 'Flexible catalytic site conformations implicated in modulation of HIV-1 protease autoprocessing reactions', *Retrovirology*. BioMed Central Ltd, 8(1), p. 79. doi: 10.1186/1742-4690-8-79.

Huang, M. *et al.* (1995) 'p6Gag is required for particle production from full-length human immunodeficiency virus type 1 molecular clones expressing protease.', *Journal of virology*, 69(11), pp. 6810–8.

Iro, M. *et al.* (2009) 'A reporter cell line for rapid and sensitive evaluation of hepatitis C virus infectivity and replication', 83, pp. 148–155. doi: 10.1016/j.antiviral.2009.04.007.

Irshad, M. *et al.* (2016) 'Multiplex qPCR for serodetection and serotyping of hepatitis viruses: A brief review', *World Journal of Gastroenterology*, 22(20), pp. 4824–4834. doi: 10.3748/wjg.v22.i20.4824.

Kamiyama, D. *et al.* (2016) 'fluorescent protein', *Nature Communications*. Nature Publishing Group, 7, pp. 1–9. doi: 10.1038/ncomms11046.

Kanno, A. *et al.* (2007) 'Cyclic Luciferase for Real-Time Sensing of Caspase-3 Activities in Living Mammals´*Angewandte Chemie International Edition*, 46(40), 7595–7599. doi: 10.1002/anie.200700538.

Karacostas, V. *et al.* (1993) 'Overexpression of the hiv-1 gag-pol polyprotein results in intracellular activation of hiv-1 protease and inhibition of assembly and budding of virus-like particles', *Virology*, pp. 661–671. doi: 10.1006/viro.1993.1174.

Kenneth A. Giuliano, D. L. T. (1998) 'Fluorescent-proteinbiosensors: New tools for drug discovery', *Trends in Biotechnology*, 16, pp. 135–140. doi:10.1016/S0167-7799(97)01166-9.

Kim, J. H. *et al.* (2013) 'In-Cell Protease Assay Systems Based on Trans-Localizing

Molecular Beacon Proteins Using HCV Protease as a Model System',*PLoS ONE* 8(3) e59710. doi: 10.1371/journal.pone.0059710.

Konvalinka, J. a N. *et al.* (2001) 'Cell-Based Fluorescence Assay for Human Immunode ciency Virus Type 1 Protease Activity, *Microbiology*, 45(9), pp. 2616–2622. doi: 10.1128/AAC.45.9.2616.

LaBarre, D. D. and Lowy, R. J. (2001) 'Improvements in methods for calculating virus titer estimates from TCID50and plaque assays', *Journal of Virological Methods*, 96(2), pp. 107–126. doi: 10.1016/S0166-0934(01)00316-0.

Laco, G. S. (2015) 'HIV-1 protease substrate-groove: Role in substrate recognition and inhibitor resistance', *Biochimie*. Elsevier Ltd, 118, pp. 90–103. doi: 10.1016/j.biochi.2015.08.009.

Lee, Y. F. *et al.* (2003) 'Development of a cell-based assay for monitoring hepatitis C virus NS3/4A protease activity', *Acta Virologica*, 52(3), pp. 133–141. doi: 10.1016/S0003-2697(03)00053-8.

Leopold, P. L. *et al.* (1998) 'Fluorescent virions: dynamic tracking of the pathway of adenoviral gene transfer vectors in living cells.', *Human gene therapy*, 9(3), pp. 367–78. doi: 10.1089/hum.1998.9.3-367.

Lion, T. (2014) 'Adenovirus infections in immunocompetent and immunocompromised patients', *Clinical Microbiology Reviews*, 27(3), pp. 441–462. doi: 10.1128/CMR.00116-13.

Livak, K. J. and Schmittgen, T. D. (2001) 'Analysis of Relative Gene Expression Data Using Real- Time Quantitative PCR and the $2^{-\Delta\Delta Ct}$ Method', *METHOD,S* 25(4), pp. 402–408. doi: 10.1006/meth.2001.1262.

Loeb, D. D. *et al.* (1989) 'Complete mutagenesis of the HIV-1 protease', *Nature*, 340(6232), pp. 397–400. doi: 10.1038/340397a0.

Louis, N., Evelegh, C. and Graham, F. L. (1997) 'Cloning and Sequencing of the Cellular – Viral Junctions from the Human Adenovirus Type 5 Transformed 293 Cell Line', *DNA Sequence*, 429(233), pp. 423–429.

Lupas, A. (1996) 'Coiled coils: new structures and new functions', *Trends in Biochemical Sciences*, 21(10), pp. 375–382. doi: 10.1016/S0968-0004(96)90126-7.

Lutz, A. *et al.* (2005) 'Virus-inducible reporter genes as a tool for detecting and quantifying influenza A virus replication', *Journal of Virological Methods*, 126(1-2), pp. 13–20. doi: 10.1016/j.jviromet.2005.01.016.

Mangel, W. F. *et al.* (1993) 'Viral DNA and a viral peptide can act as cofactors of adenovirus virion proteinase activity', *Nature*, 361(6409), pp. 274–275. doi: 10.1038/361274a0.

Mason, J. M. and Arndt, K. M. (2004) 'Coiled coil domains: Stability, specificity, and biological implications', *ChemBioChem*, 5(2), pp. 170–176. doi: 10.1002/cbic.200300781.

Matthews, R. E. F. (1979) 'The Classification and Nomenclature of Viruses', *Intervirology*, 11(3), pp. 133–135. doi: 10.1159/000149025.

McSharry, J. and Costantino, R. (1990) 'Rapid detection of herpes simplex virus in clinical samples by flow cytometry after amplification in tissue culture.', *Journal of clinical Microbiology*,

28(8), pp. 1864–1866.

Mcsharry, J. J. (1994) 'Uses of flow cytometry in virology', *Clinical Microbiology Reviews*, 7(4), pp. 576–604. doi: 10.1128/CMR.7.4.576.

Miklo, G. *et al.* (2006) 'Characterization of the murine leukemia virus protease and its comparison with the human immunodeficiency virus type 1 protease', *The Journal of General Virology*, pp. 1321–1330. doi: 10.1099/vir.0.81382-0.

Miller, M. *et al.* (1989) 'Structure of complex of synthetic HIV-1 protease with a substrate-based inhibitor at 2.3 A resolution.', *Science (New York, N.Y.)*, 246(4934), pp. 1149–52. doi: 10.1126/science.2686029.

Miyawaki, a *et al.* (1997) 'Fluorescent indicators for Ca2+ based on green fluorescent proteins and calmodulin.', *Nature*, 388(6645), pp. 882–887. doi: 10.1038/42264.

Mountain, A. (2000) 'Gene therapy: The first decade', *Trends in Biotechnology*, 18(3), pp. 119–128. doi: 10.1016/S0167-7799(99)01416-X.

Muralidharan, V. and Muir, T. W. (2006) 'Protein ligation: An enabling technology for the biophysical analysis of proteins', *Nature Methods*, 3(6), pp. 429–438. doi: 10.1038/nmeth886.

Naldini, L. *et al.* (1996) 'In vivo gene delivery and stable transduction of non dividing cells by a lentiviral vector', *Science*, 272(13), pp. 263–267.

Navia, M. A. *et al.* (1989) 'Three-dimensional structure of aspartyl protease from human immunodeficiency virus HIV-1.', *Nature*, pp. 615–620. doi: 10.1038/337615a0.

Ng, P. and Graham, F. L. (2002) 'Chapter 4 – Adenoviral Vector Construction I: Mammalian Systems', *Adenoviral Vectors for Gene Therapy*, pp. 71–104. doi: 10.1016/B978-012199504-1/50005-5.

Nguyen, H. L. T. *et al.* (2015) 'An efficient procedure for the expression and purification of HIV-1 protease from inclusion bodies', *Protein Expression and Purification*. Elsevier Inc., 116, pp. 59–65. doi: 10.1016/j.pep.2015.07.011.

Orm , M. *et al.* (1996) 'Crystal Structure of the Aequorea victoria Green Fluorescent Protein', *Science*, 273(5280), pp. 1392–1395. doi: 10.1126/science.273.5280.1392.

Partin, K. *et al.* (1991) 'Deletion of sequences upstream of the proteinase improves the proteolytic processing of human immunodeficiency virus type 1.', *Proceedings of the National Academy of Sciences of the United States of America*, 88(11), pp. 4776–4780.

Pauwels, K. *et al.* (2009) 'State-of-the-Art Lentiviral Vectors for Research Use: Risk Assessment and Biosafety Recommendations', *Current Gene Therapy*, 9(6), pp. 459–474. doi: 10.2174/156652309790031120.

Pearl, L. H. and Taylor, W. R. (1987) 'A structural model for the retroviral proteases.', *Nature*, 329(6137), pp. 351–4. doi: 10.1038/329351a0.

Pearson, S., Jia, H. and Kandachi, K. (2004) 'China approves first gene therapy', *Nature Biotechnology*. Nature Publishing Group, 22, p. 3.

Pettit, S. C. *et al.* (1991) 'Analysis of retroviral protease cleavage sites reveals two types of cleavage sites and the structural requirements of the P1 amino acid', *Journal of Biological Chemistry*, 266(22), pp. 14539–14547.

Picanco-Castro, V., Maria de Sousa Russo-Carbolante, E. and Tadeu Covas, D. (2012) 'Advances in Lentiviral Vectors: A Patent Review', *Recent Patents on DNA & Gene Sequences*, 6(2), pp. 82–90. doi: 10.2174/187221512801327433.

Raper, S. E. *et al.* (2003) 'Fatal systemic inflammatory response syndrome in a ornithine transcarbamylase deficient patient following adenoviral gene transfer', *Molecular Genetics and Metabolism*, 80(1–2), pp. 148–158. doi: 10.1016/j.ymgme.2003.08.016.

Reddy, V. S. and Nemerow, G. R. (2014) 'Structures and organization of adenovirus cement proteins provide insights into the role of capsid maturation in virus entry and infection', *Proceedings of the National Academy of Sciences*, 111(32), pp. 11715–11720. doi: 10.1073/pnas.1408462111.

Rizzo, M. A., Davidson, M. W. and Piston, D. W. (2009) 'Fluorescent protein tracking and detection: Fluorescent protein structure and color variants', *Cold Spring Harbor Protocols*, 4(12). doi: 10.1101/pdb.top63.

Robbins, P. D. and Ghivizzani, S. C. (1998) 'Viral Vectors for Gene Therapy', *Pharmacology & Therapeutics*, 80(1), pp. 35–47. doi: 10.1016/S0163-7258(98)00020-5.

Roberts, N. *et al.* (1990) 'Rational design of peptide-based HIV proteinase inhibitors', *Science*, 248(4953), pp. 358–361. doi: 10.1126/science.2183354.

Robillard, N. *et al.* (1997) 'Development of a Method for Direct Quantification of Cytomegalovirus Antigenemia by Flow Cytometry', *Journal of Clinical Microbiology*, 35(10), pp. 2665–2669.

Rodrigues, A. F. *et al.* (2014) 'Cellular targets for improved manufacturing of virus-based biopharmaceuticals in animal cells', *Trends in Biotechnology*. Elsevier Ltd, 32(12), pp. 602–607. doi: 10.1016/j.tibtech.2014.09.010.

Rodrigues, A. F. *et al.* (2015) 'Viral vaccines and their manufacturing cell substrates: New trends and designs in modern vaccinology', *Biotechnology Journal*, 10(9), pp. 1329–1344. doi: 10.1002/biot.201400387.

Rowe, W. P. *et al.* (1953) 'Isolation of a Cytopathogenic Agent from Human Adenoids Undergoing Spontaneous Degeneration in Tissue Culture', *Proceedings of the Society for Experimental Biology and Medicine*. SAGE Publications, 84(3), pp. 570–573. doi: 10.3181/00379727-84-20714.

Schulze-Horsel, J., Genzel, Y. and Reichl, U. (2008) 'Flow cytometric monitoring of influenza A virus infection in MDCK cells during vaccine production', *BMC Biotechnology*, 8, pp. 1–12. doi: 10.1186/1472-6750-8-45.

Seward, H. E. and Bagshaw, C. R. (2009) 'The photochemistry of fluorescent proteins: implications for their biological applications', *Chemical Society Reviews*, 38(10), p. 2842. doi: 10.1039/b901355p.

Shekhawat, S. S. *et al.* (2009) 'An Autoinhibited Coiled-Coil Design Strategy for Split-Protein Protease Sensors', (Figure 1), pp. 15284–15290.

Shimomura, O. (1979) 'Structure of the chromophore of Aequorea green fluorescent protein', *FEBS Letters*, pp. 220–222. doi: 10.1016/0014-5793(79)80818-2.

Shoeman, R. L. *et al.* (1990) 'Human immunodeficiency virus type 1 protease cleaves the intermediate filament proteins vimentin, desmin, and glial fibrillary acidic protein.', *Proceedings of the National Academy of Sciences of the United States of America*, 87(16), pp. 6336–40. doi: 10.1073/PNAS.87.16.6336.

Shoeman, R. L. *et al.* (1993) 'Cleavage of human and mouse cytoskeletal and sarcomeric proteins by human immunodeficiency virus type 1 protease. Actin, desmin, myosin, and tropomyosin.', *The American journal of pathology*, 142(1), pp. 221–230.

Shoeman, R. L. *et al.* (2001) 'Amino-terminal polypeptides of vimentin are responsible for the changes in nuclear architecture associated with human immunodeficiency virus type 1 protease activity in tissue culture cells.', *Molecular biology of the cell*, 12(1), pp. 143–54. doi: 10.1091/mbc.12.1.143.

Thomas, C. E., Ehrhardt, A. and Kay, M. A. (2003) 'Progress and problems with the use of viral vectors for gene therapy', *Nature Reviews Genetics*. Nature Publishing Group, 4, p. 346.

Tien, C. *et al.* (2018) 'Context-dependent autoprocessing of human immunodeficiency virus type 1 protease precursors', *Plos One*, 13(1), p. e0191372. doi: 10.1371/journal.pone.0191372.

To, T. L. *et al.* (2016) 'Rational Design of a GFP-Based Fluorogenic Caspase Reporter for Imaging Apoptosis In Vivo', *Cell Chemical Biology*, 23(7), pp. 875–882. doi: 10.1016/j.chembiol.2016.06.007.

Todd, M. J. and Freire, E. (1999) 'The effect of inhibitor binding on the structural\rstability and cooperativity of the HIV-1 protease.', *Proteins*, 36(2), pp. 147–156.

Todd, M. J., Semo, N. and Freire, E. (1998) 'The structural stability of the HIV-1 protease.', *Journal of molecular biology*, 283(2), pp. 475–488. doi: 10.1006/jmbi.1998.2090.

Tomás, H. A. *et al.* (2018) 'LentiPro26: novel stable cell lines for constitutive lentiviral vector production', *Scientific Reports*, 8(1), p. 5271. doi: 10.1038/s41598-018-23593-y.

Tóth, G. and Borics, A. (2006) 'Flap opening mechanism of HIV-1 protease', *Journal of Molecular Graphics and Modelling*, 24(6), pp. 465–474. doi: 10.1016/j.jmgm.2005.08.008.

Turner, B. G. and Summers, M. F. (1999) 'Structural biology of HIV [Review]', *Journal of Molecular Biology*, 285(1), pp. 1–32.

Watanabe, N. *et al.* (2015) 'Re-examination of regulatory opinions in Europe: possible contribution for the approval of the first gene therapy product Glybera', *Molecular Therapy - Methods and Clinical Development*. American Society of Gene & Cell Therapy, 2, p. 14066. doi: 10.1038/mtm.2014.66.

Watts, J. M. *et al.* (2009) 'Genome', *Nature*, 460(7256), pp. 711–716. doi:10.1038/nature08237.Architecture.

Waye, M. M. Y. and Sing, C. W. (2010) 'Anti-viral drugs for human adenoviruses', *Pharmaceuticals*, 3(10), pp. 3343–3354. doi: 10.3390/ph3103343.

Webster, A., Hay, R. T. and Kemp, G. (1993) 'The adenovirus protease is activated by a virus-coded disulphide-linked peptide', *Cell*, 72(1), pp. 97–104. doi: 10.1016/00928674(93)90053-S.

Wickham, T. J. *et al.* (1993) 'Integrins αvβ3and αvβ5promote adenovirus internalization but

not virus attachment', *Cell*, 73(2), pp. 309–319. doi: 10.1016/0092-8674(93)90231-E.

Wirth, T., Parker, N. and Ylä-Herttuala, S. (2013) 'History of gene therapy', *Gene*. Elsevier B.V., 525(2), pp. 162–169. doi: 10.1016/j.gene.2013.03.137.

Wlodawer, A. *et al.* (1989) 'Conserved folding in retroviral proteases: crystal structure of a synthetic HIV-1 protease', *Science* 245(4918), pp. 616-621.

Wlodawer, A. and Vondrasek, J. (1998) 'Inhibitors of HIV-1 protease: a major success of structure-assisted drug design.' *Annual Review of Biophysics and Biomolecular Structure*. 1998;27:249-84.

Wong, A. A. *et al.* (2016) 'Development of a multiplex real-time PCR for the simultaneous detection of herpes simplex and varicella zoster viruses in cerebrospinal fluid and lesion swab specimens', *Journal of Virological Methods*. Elsevier B.V., 229, pp. 16–23. doi: 10.1016/j.jviromet.2015.12.009.

Yan, X. *et al.* (2005) 'Multiplexed flow cytometric immunoassay for influenza virus detection and differentiation', *Analytical Chemistry*, 77(23), pp. 7673–7678. doi: 10.1021/ac0508797.

Zhang, J. *et al.* (2013) 'Visualization of caspase-3-like activity in cells using a genetically encoded fluorescent biosensor activated by protein cleavage', *Nature Communications*. Nature Publishing Group, 4, pp. 1–13. doi: 10.1038/ncomms3157.

Zubieta, C. *et al.* (2005) 'The structure of the human adenovirus 2 penton', *Molecular Cell*, 17(1), pp. 121–135. doi: 10.1016/j.molcel.2004.11.041.

Annexes

Table A.1- Primers for plasmid construction

Final plasmid	Insert			Vector
	Fragment size	Source	Primers	
pRRLSIN.CMV.mCherry.HIV1Pr.WPRE	731bp	pPURO_mCHERRY	**F**-CGTCAGATCCGCTAGCCGCCACCATGG	*pRRLSIN.CMV.GFPS10.IRES.Zeo.WPRE.v2* opened with Nhe I and SalI
			R- CTTGTACAGCTCGTCCATGC	
	460bp	pMDLg/pRRE	**F**-GACGAGCTGTACAAGTGGGGAAGAGAC	
			R- GAGGTTGATTGTCGACTTATTTTGGGC	
pRRLSIN.CMV.mCherry.HIV1PrD25N.WPRE	731bp	pPURO_mCHERRY	**F**-CGTCAGATCCGCTAGCCGCCACCATGG	*pRRLSIN.CMV.GFPS10.IRES.Zeo.WPRE.v2* opened with Nhe I and SalI
			R- CTTGTACAGCTCGTCCATGC	
	460bp	pMDLg/RRED25N	**F**-GACGAGCTGTACAAGTGGGGAAGAGAC	
			R- GAGGTTGATTGTCGACTTATTTTGGGC	
pRRLSIN.CMV.eGSGIFLETSL.v2.IRES.Puro.WPRE	103bp	pUC57.eLRGAG-GFPS11	**F**-TTTCTGGAAACCAGCCTG	*pRRLSIN.CMV.GFPS10.IRES.Puro.WPRE.v2* opened with Nhe I and BamHI
			R- TACAATAGAGTGCGGGTGTTCTAC	
	227bp	pUC57.eLRGAG-GFPS11	**F**-GGTGATGCCAGCCAGCGGCGTT	
			R- CAGGCTGGTTTCCAGAAAGATGCCGCTGCC	
pRRLSIN.CMV.eIRKILFLDG.v2.IRES.Puro.WPRE	103bp	pUC57.eLRGAG-GFPS11	**F**-ATCCTGTTCCTGGACGGC	*pRRLSIN.CMV.GFPS10.IRES.Puro.WPRE.v2* opened with Nhe I and BamHI
			R- TACAATAGAGTGCGGGTGTTCTAC	
	224bp	pUC57.eLRGAG-GFPS11	**F**-GCCGTCCAGGAACAGGATCTTCCGGAT	
			R- GGTGATGCCAGCGGCGTT	
pRRLSIN.CMV.cIRKILFLDG-GFPS11.IRES.Puro.WPRE	451bp	pUC57.cLRGAG-GFPS11	**F**-ATCCTGTTCCTGGACGGC	*pRRLSIN.CMV.GFPS10.IRES.Puro.WPRE.v2* opened with Nhe I and BamHI
			R- AGGGACCACATGGTGCTGC	
	167bp	pUC57.cLRGAG-GFPS11	**F**-GTTGAAGCAGTTGCTGGCG	
			R- GCCGTCCAGGAACAGGATCTTCCGGAT	

Table A.2 – Primers for qPCR

Target/Gene	5' to 3' sequence
Ribossomal protein L22 (RPL22)	F-CTGCCAATTTTGAGCAGTTT
	R-CTTTGCTGTTAGCAACTACGC
HIV-1 Long Terminal Repeat (LTR)	F-CTGCCAATTTTGAGCAGTTT
	R-GCTAGAGATTTTCCACACTGA
Woodchuck Hepatitis Virus Post-Transcriptional Regulatory Element (WPRE)	F-ACTGTGTTTGCTGACGCAAC
	R-ACAACACCACGGAATTGTCA